Organisms Diversity & Evolution (2022) 22:61–92
https://doi.org/10.1007/s13127-021-00517-9

ORGANISMS DIVERSITY & EVOLUTION

ORIGINAL ARTICLE

Molecular investigation and description of *Iberozospeum* n. gen., including the description of one new species (Eupulmonata, Ellobioidea, Carychiidae)

Jeannette Kneubühler[1,2] · Adrienne Jochum[1,2,3] · Carlos E. Prieto[4] · Eike Neubert[1,2]

Received: 30 April 2021 / Accepted: 30 August 2021 / Published online: 5 November 2021

Abstract

The subterranean realm of the Cantabrian-Pyrenean region of northern Spain harbours a rich diversity of *Zospeum*. Due to their tiny size and the difficulty of finding them alive, scarce animal material has been available for scientific investigation. Recent investigations of *Zospeum* shells have provided valuable, but limited insights towards our understanding of the evolutionary processes occurring within this taxon in northern Spain. In an integrative study, we investigate 57 populations of *Zospeum* from northern Spanish caves using two mitochondrial (COI and 16S) and two nuclear markers (H3 and 5.8 S rRNA + ITS2). Revealed is a separate radiation of the northern Spanish species for which the new genus, *Iberozospeum,* is proposed. The independent radiation of Dinaric *Zospeum* from that of northern Spain justifies the designation of *Iberozospeum* n. gen. Morphological evidence is provided via histological analysis of *Iberozospeum vasconicum* and SEM analyses of radulae of eastern Alpine, Dinaric and Iberian species. Important differences in morphological structure and character states are presented, including the first view of the sexually mature female and the presence of the giant albumen gland in an individual of the subterranean, troglobitic Carychiidae. Significant differences are revealed in superficial crystallographic structure of the columellar lamellae, the morphology of the columellar muscle and in the radula. Radular ribbon length, ribbon broadness, straightness of the ribbon base and cusp configuration are distinctive in the Iberian species. One new species is described corroborated by genetic and morphological characters.

Keywords Cave-dwelling species · Cryptic diversity · Histology · Intraspecific variability · Microgastropods · Subterranean land snail

Introduction

Tiny subterranean snails of the genus *Zospeum* (Bourguignat, 1856), are known to inhabit the broad network of caves underlying the Pyrenean-Cantabrian region of northern Spain (Fig. 1). Although recent collection efforts have provided significant finds, many new discoveries have remained parked in the lab due to doubts and complications regarding the taxonomic status of the oldest-described species from Spain, *Iberozospeum schaufussi* (von Frauenfeld, 1862; Jochum et al., 2019). Only until recently were these taxonomic issues clarified such that the description of new species could proceed unhindered in a region known to harbour rich "*Zospeum*" diversity (Jochum et al., 2019). We emphasise that northern Spanish material molecularly assessed by Weigand et al. (2013) as cf. *Z. suarezi* (Gittenberger, 1980) and deposited in the BOLD data base under this name was revised (Jochum et al., 2019) and is now in sync with this investigation, *I. schaufussi* (von Frauenfeld, 1862). Caves harbouring two to three different morphotypes are considered not unusual (Alonso et al., 2018). Despite this suggested richness, only eight species have been formally described, including *I. schaufussi* (von Frauenfeld, 1862), *I. bellesi* (Gittenberger, 1973), *I. biscaiense* (Gómez & Prieto, 1983), *I. vasconicum* (Prieto et al., 2015 in Jochum et al., 2015a), *I. zaldivarae* (Prieto et al.,

✉ Jeannette Kneubühler
jeannette.kneubuehler@nmbe.ch

1 Natural History Museum Bern, 3005 Bern, Switzerland

2 Institute of Ecology and Evolution, University of Bern, 3012 Bern, Switzerland

3 Senckenberg Research Institute and Natural History Museum, 60325 Frankfurt am Main, Germany

4 Departamento de Zoología Y Biología Celular Animal, Facultad de Ciencia Y Tecnología, Universidad del País Vasco (UPV/EHU), Apdo.644, 48080 Bilbao, Spain

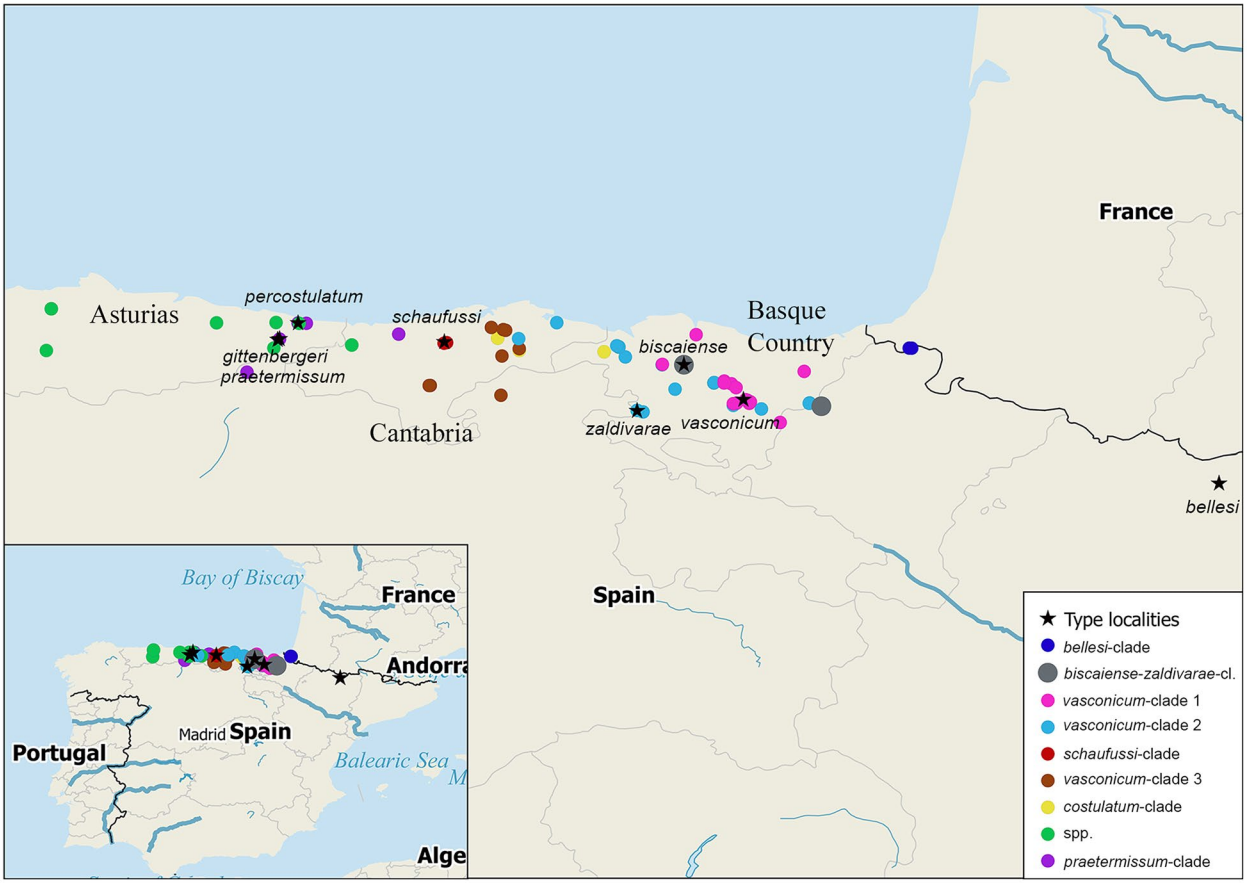

Fig.1 Sampling locations of *Iberozospeum* specimens from northern Spanish caves grouped into clades named by province of origin and designated by coloured circles; stars represent the type localities of the hitherto known species

2015 in Jochum et al., 2015a), *I. percostulatum* (Alonso et al., 2018) and recently, *I. gittenbergeri* (Jochum et al., 2019) and *I. praetermissum* (Jochum et al., 2019).

Weigand et al. (2013) presented the first phylogenetic study incorporating Iberian "*Zospeum*" species, whereby nine populations of "*Zospeum*" are clustered into six evolutionary lineages (EL), with those from the Cantabrian Mountains being monophyletic. This study and additional phylogenetic investigations have since demonstrated the high incidence of intraspecific variability and cryptic diversity in Iberian, Eastern Alpine (Kruckenhauser et al., 2019; Weigand et al., 2011) and Dinaride (Inäbnit et al., 2019) *Zospeum* species.

In order to further understand zospeid evolutionary history in caves of northern Spain, we molecularly assess recent finds encompassing 57 populations. Anatomical perspectives of zospeid radulae and organ systems remain rare and few in number. Seven studies are known so far (see Jochum, 2011; Jochum et al., 2015b; Inäbnit et al., 2019). By studying histological sections of topotypic *I. vasconicum,* topotypic *Z. isselianum* (Pollonera, 1887) and *Z. amoenum* (von Frauenfeld, 1856) (see Jochum et al. 2015b) and *Z. spelaeum* (Rossmässler, 1839), we compare the presence of specific structures and character states in the visceral mass of one northern Spanish and three Dinaride taxa. We additionally describe significant differences in radular morphology and crystallographic structure on the columellar lamellae using scanning electron microscopy (SEM). Together, these investigations support the erection of the new genus, *Iberozospeum*.

Material and methods

Material is housed in the following collections:

AJC: Adrienne Jochum Collection, Kelkheim, Germany.
CAA: Collection of Alvaro Alonso, Spain.
CSQS: Collection of Sergio Quiñonero-Salgado, Spain.
MHNG: Muséum histoire naturelle Gèneve, Geneva, Switzerland.

MNCN: Museo Nacional de Ciencias Naturales, Madrid, Spain.
MZB: Museu de Ciències Naturals (Zoologia) de Barcelona, Barcelona, Spain.
NHMW: Naturhistorisches Museum, Wien, Vienna, Austria.
NMBE: Naturhistorisches Museum der Burgergemeinde Bern, Bern, Switzerland.
RMNH: Naturalis Biodiversity Center (formerly Rijks-Museum van Natuurlijke Historie), Leiden, The Netherlands.
ZUPV/FC: Colección de Fauna Cavernícola (Departamento de Zoología) de la Universidad del País Vasco-Euskal Herriko Unibertsitatea, Bilbao, Spain.

Individuals investigated in the molecular study

Individuals used for DNA sequence analyses were collected primarily by Carlos Prieto, Alvaro Alonso Suárez and Sergio Quiñonero-Salgado and additional collectors in caves from Asturias province to as far east as Navarra during the years 1987–2018. A total of 67 individuals were included. Sampling locations and the GenBank accession numbers for the obtained mtDNA (COI, 16S) and nDNA (H3, 5.8 S rRNA + ITS2) sequences are given in Table 1. Molecular analyses include the outgroup species *Zospeum spelaeum* (Rossmässler, 1839), *Zospeum exiguum* (Kuščer, 1932), *Zospeum manitaense* (Inäbnit et al., 2019), *Zospeum robustum* (Inäbnit et al., 2019), *Zospeum frauenfeldii* (Freyer, 1855), *Zospeum obesum* (von Frauenfeld, 1854) and *Zospeum pretneri* (Bole, 1960) from the Dinaric Alps (Inäbnit et al., 2019; Weigand et al., 2013). Additionally, sequences of *I. vasconicum* (No. 151 in Weigand et al., 2013), *I. schaufussi* (as *I. suarezi*, No. 140 in Weigand et al., 2013) and *I. zaldivarae* (No. 162 and 163 in Weigand et al., 2013) from their type localities were included. All images and DNA extracts of the specimens investigated in this study are housed in the Natural History Museum Bern (NMBE), Bern, Switzerland.

DNA extraction, PCR amplification, and sequence determination

Live specimens were preserved in 80% ethanol. Before DNA extraction, every specimen was imaged under sterile conditions from frontal and apical view with a Leica DFC425 microscope camera using the image-processing program (IMS Client V15Q4, Imagic, Switzerland). For total DNA extraction, the Qiagen Blood and Tissue Kit (Qiagen; Hilden, Germany) was used. Each specimen was placed in a mix of 180 µl ATL buffer and 20 µl Proteinase K. It was then incubated for ca. 2 h at 56 °C in a heater (Labnet, Vortemp 56, witec AG, Littau, Switzerland). For subsequent DNA extraction, 200 µl Buffer AL was added. The mixture was vortexed and incubated at 56 °C for 10 min. Ethanol of 200 µl (100%) was added and vortexed again. The mixture was pipetted in a DNeasy Mini spin column placed in a 2 ml collection tube and centrifuged at 8000 rpm (Centrifuge 5424, Eppendorf) for 1 min. The spin column was placed in a new 2 ml collection tube and 500 µl Buffer AW1 was added. It was centrifuged for 1 min at 8000 rpm. The spin column was placed in a new 2 ml collection tube, and 500 µl Buffer AW2 was added. It was centrifuged for 3 min at 14,000 rpm. Afterwards, the spin column was transferred to a new 1.5 ml Eppendorf tube. The DNA was then eluted by adding 200 µl Buffer AE. It was incubated for 1 min at room temperature (ca. 23 °C) and centrifuged for 1 min at 8000 rpm.

In this study, two mitochondrial (mtDNA) markers (COI and 16S) and two nuclear (nDNA) markers (H3 and 5.8 S rRNA + ITS2) were investigated. PCR mixtures consisted of 12.5 µl GoTaq G2 HotStart Green Master Mix (Promega M7423), 4.5 µl ddH_2O, 2 µl forward and reverse primer each and 4 µl DNA template. In Table 2 the respective primer pairs for the PCR are listed. The following PCR cycles were used as follows: for COI the admixture was heated 2 min at 94 °C, followed by 35 cycles of 1 min at 95 °C, 1 min at 40 °C and 1 min at 72 °C and, finally, 5 min at 72 °C; for 16S the admixture was heated 5 min at 95 °C, followed by 45 cycles of 30 s at 95 °C, 30 s at 48 °C and 45 s at 72 °C and, finally, 5 min at 72 °C; for H3 the admixture was heated 3 min at 95 °C, followed 40 cycles of 1 min at 95 °C, 1 min at 42 °C and 1 min at 72 °C and, finally, 10 min at 72 °C; and for 5.8 S rRNA + ITS2 the admixture was heated 1 min at 96 °C, followed by 45 cycles of 30 s at 94 °C, 30 s at 50 °C and 1 min at 72 °C and, finally, 10 min at 72 °C (SensoQuest Tabcyclet and Techne TC-512, witec AG, Littau, Switzerland). The purification and sequencing of the PCR products were performed by LGC (LGC Genomics Berlin, Germany).

Specimens collected in 2011 or later could be successfully sequenced. Since the DNA content in older specimens was too low for any analyses, sequences of those specimens could not be included in our study. Long-term storage in ethanol proved to be problematic for the successful sequencing of such tiny snails (< 1.5 mm).

Phylogenetic analyses

The software package Geneious v9.1.8 (Biomatters Ltd) was used for sequence processing and editing. Maximum likelihood (ML) topology was estimated with the Geneious RAxML plug-in (Stamatakis, 2006) using rapid bootstrapping setting to compute the best scoring ML tree and 1500 bootstrapping replicates. The protein-coding gene fragments of COI was defined in two data blocks. The first and third codon positions were defined as one block and the second

Table 1 Sampled northern Spanish caves with their geographic location and the GenBank accession numbers for the analysed mtDNA (COI, 16S) and nDNA (H3, 5.8 S rRNA + ITS2) sequences

NMBE-No	ZUPV-No	Cave and Province	Latitude	Longitude	Altitude [m]	GenBank accession number COI	GenBank accession number 16S	GenBank accession number H3	GenBank accession number ITS2
540551_1	1847	Akaitz Txiki (Gipuzkoa)	42.9818	−2.0925	824	MW626838	MW621911	MW622169	MW621272
540552_1	2039	Azkillar (Bizkaia)	43.0882	−2.5912	1030	MW626839	MW621915	MW622173	MW621275
540552_3	2039	Azkillar (Bizkaia)	43.0882	−2.5912	1030	MW626841	MW621917	MW622175	MW621277
540553_1	1066	Elorrea (Bizkaia)	43.0538	−2.7956	1059	-	MW621919	MW622177	-
540554_4	1309	Arrikrutz (Gipuzkoa)	42.9988	−2.4265	495	-	MW621920	MW622181	MW621282
540555_2	937	Basotxo (Navarra)	42.8798	−2.246	705	-	-	MW622183	-
540556_1	874	Hatxondo (Bizkaia)	43.1835	−2.862	300	-	-	MW622184	-
557136	4885	Herreria (Asturias)	43.39784	−4.75967	50	-	MW621921	MW622188	MW621284
557138	4702	Baja (Cantabria)	43.40163	−3.41371	51	MW626842	MW621922	MW622189	MW621285
557140	4862	Collubina (Asturias)	43.39841	−4.72264	45	MW626843	MW621923	MW622190	MW621286
557142	3671	Cumbre (Asturias)	43.26893	−4.89248	1761	-	MW621924	MW622191	-
557144	4136	Udias (Cantabria)	43.34163	−4.23989	109	MZ620729	MW621925	MW622192	MW621287
557146	3820	Montosas (Cantabria)	43.22731	−3.70042	725	MW626844	MW621926	MW622193	MW621288
557150	3405	Txomenkoba (Gipuzkoa)	42.98131	−2.47352	810	MW626845	MW621927	MW622194	MW621289
557152	3758	San Valerio (Gipuzkoa)	43.08203	−2.50105	444	MW626846	MW621928	MW622195	MW621290
557154	3849	Penpelin (Gipuzkoa)	43.062	−2.47655	690	MW626847	MW621929	MW622196	MW621291
557156	3856	Artegi (Bizkaia)	43.09628	−2.53847	540	MW626848	MW621930	MW622197	MW621292
557158	4601	Saiturri-2 (Gipuzkoa)	42.96902	−2.49111	1063	MW626849	MW621931	MW622198	MW621293
557160	4757	Urkoba (Gipuzkoa)	42.97802	−2.49103	1020	-	-	MW622199	MW621294
557162	4821	Perusaroi-1 (Gipuzkoa)	42.95026	−2.34416	1156	-	MW621932	-	MW621295
557166	4990	Aizkirri (Gipuzkoa)	42.99568	−2.41728	600	MW626850	MW621933	MW622200	MW621296
557168	5005	Arlaban (Gipuzkoa)	43.08629	−2.53928	382	MW626851	MW621934	MW622201	MW621297
557174	1008	Eskatxabel-2 (Bizkaia)	43.27509	−3.0888	565	-	-	MW622202	MW621298
557178	1607	Paules (Burgos)	42.94287	−2.99363	830	MW626852	MW621935	MW622203	MW621299
557180	1740	Lejazar (Araba)	42.93484	−2.96285	836	-	MW621936	MW622204	MW621300
557182	874	Hatxondo (Bizkaia)	43.18162	−2.86335	300	-	MW621937	-	-

Table 1 (continued)

NMBE-No	ZUPV-No	Cave and Province	Latitude	Longitude	Altitude [m]	GenBank accession number COI	GenBank accession number 16S	GenBank accession number H3	GenBank accession number ITS2
557187	1847	Akaitz Txiki (Gipuzkoa)	42.97995	−2.09384	824	MW626853	MW621938	MW622205	MW621301
557188	1847	Akaitz Txiki (Gipuzkoa)	42.97995	−2.09384	824	MW626854	MW621939	MW622206	MW621302
557189	2039	Azkillar (Bizkaia)	43.08632	−2.59251	1030	MW626855	MW621940	MW622207	MW621303
557198	no number	Fuente de Estragueña (Cantabria)	43.2997	−4.6066	-	-	-	MW622208	MW621304
557200	854	San Juan-9 (Bizkaia)	43.28078	−3.1001	637	MW626856	MW621941	MW622209	-
557207	3861	Azkonar Zulueta (Gipuzkoa)	42.98749	−2.40171	790	-	MW621942	-	MW621305
557209	3904	Iritegi (Gipuzkoa)	42.9798	−2.40768	527	MW626857	MW621943	MW622210	MW621306
557211	4864	Grazal (Bizkaia)	43.22227	−3.05541	148	MW626858	MW621944	MW622211	MW621307
557213	5006	Garcia (Burgos)	43.022	−3.7057	935	MW626859	MW621945	MW622212	MW621308
557215	5091	Arrigueras (Cantabria)	43.07316	−4.07478	660	-	-	MW622213	MW621309
557217	4930	Mendikute (Gipuzkoa)	43.14687	−2.12069	710	MW626860	MW621946	MW622214	MW621310
557219	5087	Munarri Arrola (Bizkaia)	43.33892	−2.68541	63	MW626861	MW621947	MW622215	MW621311
557221	2874	Irutxin (Navarra)	42.966	−2.02518	1095	-	-	MW622216	MW621312
557223	3728	Otxas (Bizkaia)	43.18599	−2.74773	488	MW626862	MW621948	MW622217	MW621313
557225	4102	Toyo (Cantabria)	43.28468	−4.48524	190	MW626863	MW621949	MW622218	MW621314
557226	4102	Toyo (Cantabria)	43.28468	−4.48524	190	MW626864	MW621950	MW622219	MW621315
557227	4714	Cuvias Negras (Cantabria)	43.25668	−3.60984	250	-	-	MW622220	-
557229	4723	San Juan de Socueva (Cantabria)	43.26569	−3.60993	430	-	-	MW622221	MW621316
557231	3078	Valdebeci (Bizkaia)	43.24918	−3.1663	188	-	-	MW622222	MW621317
557232	4017	Princesa (Bizkaia)	43.2738	−3.08898	620	MW626865	MW621951	MW622223	MW621318
557234	3371	Lexotoa-2 (Navarra)	43.26819	−1.55843	215	MW626866	MW621952	MW622224	MW621319
557236	3323	Lezea (Navarra)	43.26853	−1.57164	210	MW626867	MW621953	MW622225	MW621320
557238	2875	Irutxin (Navarra)	42.96476	−2.03077	1095	MW626868	MW621954	MW622226	MW621321
557240	3727	Otxas (Bizkaia)	43.18165	−2.74923	488	-	MW621955	MW622227	MW621322
557242	4057	Cubija (Cantabria)	43.31812	−3.61307	269	MW626869	MW621956	MW622228	MW621323

Table 1 (continued)

NMBE-No	ZUPV-No	Cave and Province	Latitude	Longitude	Altitude [m]	GenBank accession number COI	GenBank accession number 16S	GenBank accession number H3	GenBank accession number ITS2
557244	559	Paules (Burgos)	42.94287	−2.99363	840	-	-	MW622229	MW621324
557246	5210	Valdemora (Asturias)	43.47417	−6.0556	310	MW626870	MW621957	MW622230	MW621325
557247	5302	Valdemora (Asturias)	43.47417	−6.0556	310	-	-	MW622231	MW621326
557249	4915	Llagar (Asturias)	43.25613	−6.08141	990	MW626871	MW621958	MW622232	-
557251	5211	Caleru (Asturias)	43.40077	−5.1919	80	MW626872	MW621959	MW622233	MW621327
557253	5209	Herreria (Asturias)	43.39987	−4.76584	45	MW626873	MW621960	MW622234	MW621328
557255	5208	Busecu (Leon)	43.14277	−5.03276	770	MW626874	MW621961	MW622235	-
559620	5257	Puente Inguanzo (Asturias)	43.31626	−4.86252	225	MW626875	MW621962	MW622236	MW621329
559622	5258	Zurra (Asturias)	43.40259	−4.88078	-	MW626876	MW621963	MW622237	MW621330
559624	5203	Iglesia (Cantabria)	43.36562	−3.69331	65	MW626877	MW621964	MW622238	MW621331
559626	3807	Cesareo (Cantabria)	43.32034	−3.72279	258	MW626878	MW621965	MW622239	MW621332
559628	5175	Soldados (Cantabria)	43.29725	−3.9894	370	MW626879	MW621966	MW622240	MW621333
559630	5171	Buho (Cantabria)	43.29427	−4.0028	420	MW626880	MW621967	MW622241	MW621334
559632	5213	Arrigueras (Cantabria)	43.07284	−4.0806	660	MW626881	MW621968	MW622242	MW621335
559634	5200	Murcielagos (Cantabria)	43.36159	−3.68115	70	MW626882	MW621969	MW622243	MW621336
559636	5196	Prementera (Cantabria)	43.37676	−3.75574	125	-	MW621970	MW622244	MW621337

codon position as a second block. The non-coding regions from 16S and 5.8 S rRNA + ITS2 were defined as a single data block. The nucleotide model Gamma GTR I was used. Partitionfinder-2.1.1 (Lanfear et al., 2016) was applied for searching optimal evolutionary models for the partitions using the corrected Akaike Information Criterion (cAIC).

Table 2 Primer designs used for PCR reactions

Gene	Primer	Sequence	Sequence length (bp)	Reference
COI	LCO1490	5'-GGTCAACAAATCATAAAGATATTGG-3'	680	Folmer et al. (1994)
	HCO2198	5'-TAAACTTCAGGGTGACCAAAAAATCA-3'		
16S	16S ar	5'-CGC CTG TTT ATC AAA AAC AT-3'	440	Simon et al. (1994)
	16S br	5'- CCG GTC TGA ACT CTG ATC AT -3'		
H3	H3AD	5'-ATGGCTCGTACCAAGCAGACVGC-3'	380	Colgan et al. (1998)
	H3BD	5'-ATATCCTTRGGCATRATRGTGAC-3'		
ITS2	ITS2ModA	5'-GCTTGCGGAGAATTAATGTGAA-3'	900	Bouaziz-Yahiatene et al. (2017)
	ITS2ModB	5'-GGTACCTTGTTCGCTATCGGA-3'		

Bayesian Inference (BI) was performed using Mr. Bayes v3.2.6 × 64 (Altekar et al., 2004; Huelsenbeck & Ronquist, 2001; Ronquist & Huelsenbeck, 2003) through the HPC cluster from the University of Bern (http://www.id.unibe.ch/hpc). For the concatenated data set, Partitionfinder-2.1.1 was used for finding the optimal evolutionary models for each subset with the model = all function. The Monte Carlo Markov Chain (MCMC) parameter was set as follows: starting with four chains and four separate runs for 20 million generations with a tree sampling frequency of 1000 and a burn in of 25%.

Species delimitation

The species delimitation method, Automatic Barcoding Gap Discovery (ABGD) was applied via the web browser (https://bioinfo.mnhn.fr/abi/public/abgd/abgdweb.html). The ABGD method (Puillandre et al., 2012) sorts the sequences into hypothetical species based on the barcode gap. ABGD was conducted using the COI alignment of the investigated *Iberozospeum* specimens. The input variables were chosen according to Weigand et al. (2013) and Inäbnit et al. (2019). The parameters were set as follows: Pmin = 0.001; Pmax = 0.1; Steps = 10; X = 1; Nb bins = 20; and distance: Jukes-Cantor.

Morphological analyses using scanning electron microscopy (SEM)

Radulae of the eastern Alpine and Dinaride *Zospeum* used in the comparative analyses are presented in Inäbnit et al. (2019). For reasons of space, only images of the radular ribbons of *Z. exiguum* and *Z. pretneri* are presented here (Fig. 14). Topotypic *I. vasconicum* and *I. zaldivarae* were collected by AJ for radular investigation. Individuals from the westernmost sampled caves (Asturias Province), derived from the collection of Jos Notenboom, housed at the Naturalis Biodiversity Center, Leiden, NL: RMNH.MOL.234108 Cueva de Torcona (exception from Burgos); RMNH.MOL.234147 Cueva de la Huertas; RMNH.MOL.234109 Cueva de la Foz; RMNH.MOL.234116 Cueva a Sul; RMNH.MOL.234144 Cueva de Rales.

Radulae were prepared according to Holznagel (1998), preserved in 96% ethanol and mounted onto prepared SEM aluminium stubs. The radulae were sputtered with gold (1–2 × for 60 s) in the Agar Sputter Coater (Agar Scientific, Stanstead, UK) and viewed in the high vacuum mode of the Hitachi S-4500 scanning electron microscope (15 kV, probe current 20–100 pA) using the secondary electron detector. Photographs were taken with DISS—Digital Image Scanning System 5 (Point Electronic, Halle, Germany). All processing of radulae was conducted at the Goethe University (Frankfurt, Germany).

SEM images of all Spanish shells showing crystallographic structure were made at the Naturalis Biodiversity Center (Leiden, NL) using the JEOL JSM-6480LV scanning electron microscope. Aluminium stubs were coated with gold–palladium using the Polaron Equipment LTD-E5100 SEM auto-coating sputter system. Shells of three potential new species, awaiting further investigation beyond our purposes here, derive from the J. Notenboom Collection: RMNH.MOL.234104 Cueva del Comediante; RMNH.MOL.234141 Cueva a Sul; and RMNH.MOL.234120, Cueva Refugio, Basinagre, Trucios. The former two shells were preserved in 75% ethanol by the collector (Notenboom & Meijers, 1985), and, thus, finer morphological structure is consequently eroded in these shells.

Histological sectioning and light microscopy follow Jochum et al. (2015b). Three individuals used in the comparative morphology include *Z. isselianum* (AJC 2287), Turjeva jama, Slovenia (46.2435, 13.5046); *Z. spelaeum* (AJC 848), Betalov Spodmol cave, Slovenia (45.7922, 14.1877); and *I. vasconicum* (AJC 1848), Cueva de la Ermita de Sandaili (42.9994, 2.4381).

Results

The maximum likelihood and Bayesian inference tree (Fig. 2) shows the concatenated data set (COI, 16S, H3 and 5.8 S rRNA + ITS2) of 67 specimens of species from the west European radiation from 55 caves and seven Dinaride outgroup taxa. The dataset was supplemented with genetic data from Weigand et al. (2013) of topotypic specimens of *I. vasconicum* (No. 151 in Weigand et al., 2013), *I. zaldivarae* (No. 162 and 163 in Weigand et al., 2013) and *I. schaufussi* (designated as *I. suarezi*, No. 140 in Weigand et al., 2013). The tree was rooted by two species of *Carychium* from the collection of AJ (in the NMBE). The topology reveals nine larger clades, which follow a geographic pattern (cf. Fig. 1).

The basic node separates Dinaride *Zospeum* taxa from taxa inhabiting northern Spanish caves. This node has a full ML and BI support and justifies the designation of the western *Zospeum* radiation to a separate new genus, *Iberozospeum* n. gen. The p-distances which show the numbers of base differences per site between sequences were calculated (Kumar et al., 2018). The mean p-distance from *Iberozospeum* n. gen. and *Zospeum* is 0.0767 (Table S1 in the supplementary material). The mean p-distance from *Zospeum* and *Carychium* is 0.1285. The mean p-distance of *Iberozospeum* n. gen. and *Carychium* is 0.1177.

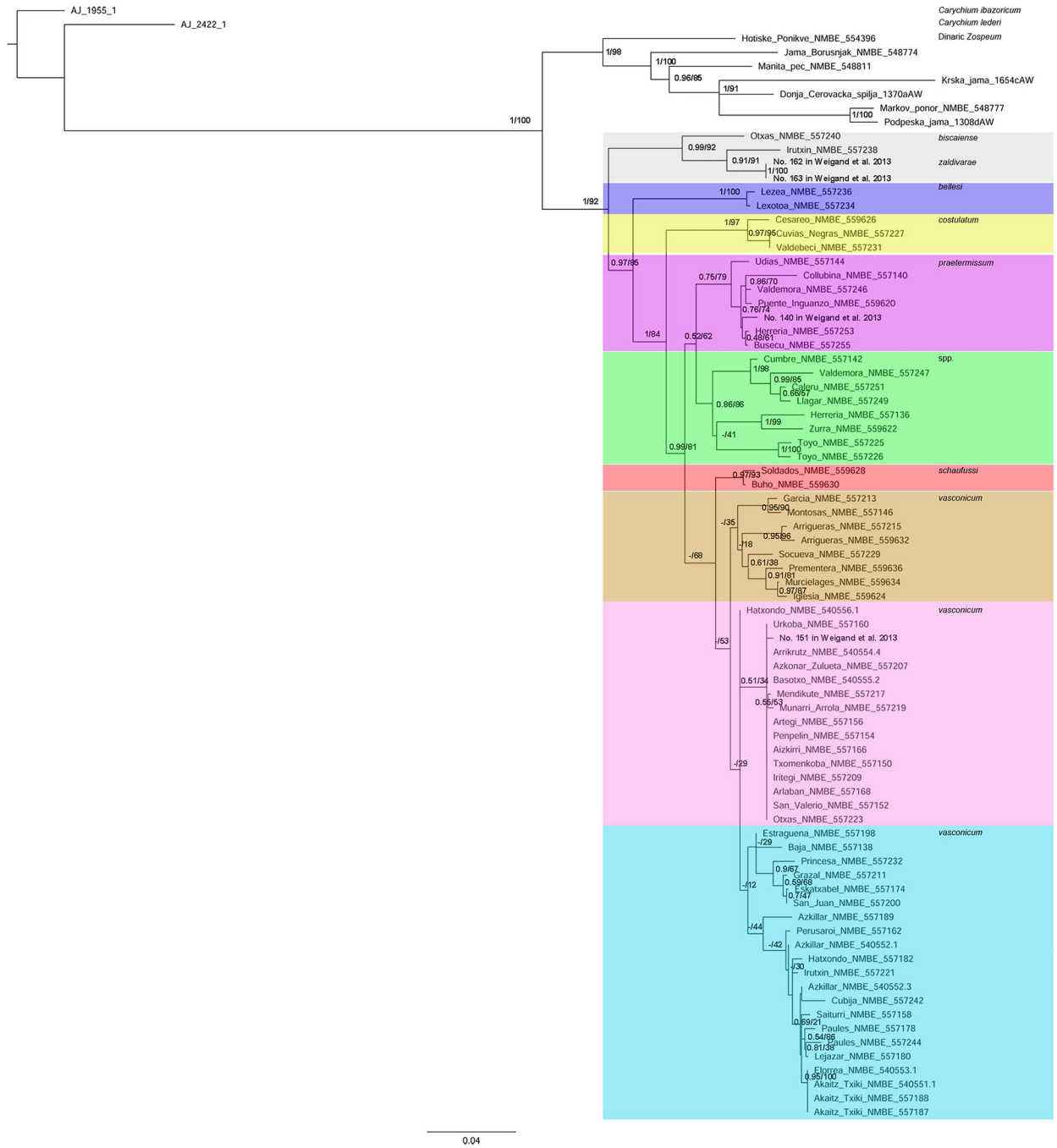

Fig. 2 Combined maximum likelihood (RAxML) and Bayesian inference (BI) tree based on concatenated data set of COI, 16S, H3 and 5.8 S rRNA + ITS2. The analysis comprises 67 individuals of northern Spanish *Iberozospeum* from 55 caves and seven Dinaride outgroup taxa. The tree was rooted by two species of *Carychium* from the collection of AJ (in the NMBE). Additionally, sequences of *I. schaufussi*, *I. vasconicum* and *I. zaldivarae* from their type localities are included. The numbers at the nodes represent the Bayesian posterior probabilities (left) and the bootstrap support values (right). The dash (-) means that the node is not supported

In order to study the effect of incomplete genetic data, a reduced set comprising 42 individuals was computed (Fig. 3). Here, only specimens were used with a complete record of all four markers. The bootstrap support values and the Bayesian posterior probabilities are over all higher in the tree with complete marker sets (Fig. 3).

The *biscaiense-zaldivarae*-clade (grey clade in Figs. 2 and 3) harbours congeners from two different caves (Otxas

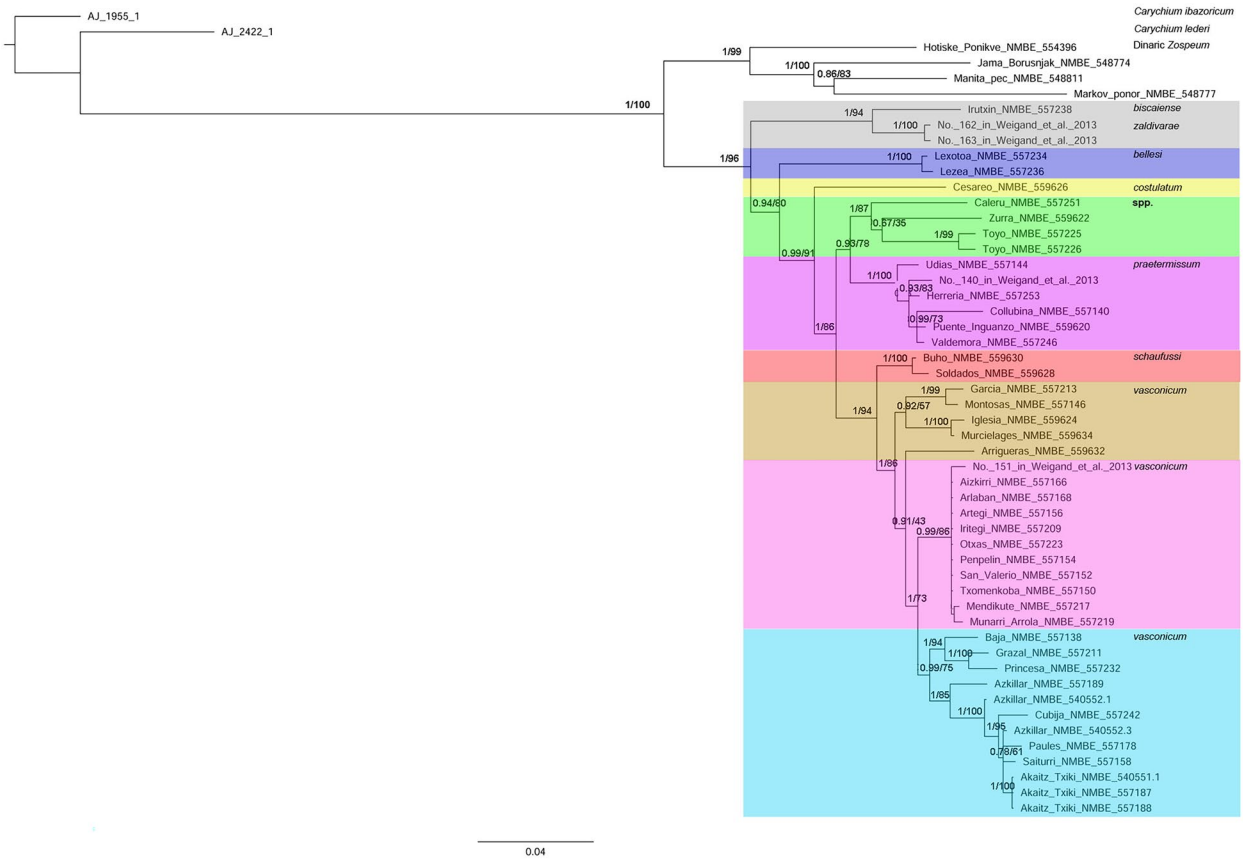

Fig. 3 Combined maximum likelihood (RAxML) and Bayesian inference (BI) tree based on concatenated data set of COI, 16S, H3 and 5.8 S rRNA + ITS2. The analysis consists of 42 individuals of northern Spanish *Iberozospeum* from 37 caves and four Dinaride outgroup taxa. Only specimens with complete marker sets are included. The tree was rooted by two species of *Carychium* from the collection of AJ (in the NMBE). Additionally, sequences of *I. schaufussi*, *I. vasconicum* and *I. zaldivarae* from their type localities are included. The numbers at the nodes represent the Bayesian posterior probabilities (left) and the bootstrap support values (right)

and Irutxin) which cluster with specimens of *zaldivarae* from the type locality (No. 162 and 163 in Weigand et al., 2013). The caves, Otxas and Irutxin, are about 100 km apart from each other and are non-contiguous. Congeners from these two caves are also found in the low-resolution *vasconicum*-clade 1 (pink clade in Figs. 2 and 3) and *vasconicum*-clade 2 (light blue clade in Figs. 2 and 3). From the external perspective, the investigated specimen (NMBE 557240) in the grey clade shows a typical *biscaiense* morph (Figs. 4a). It is found in the cave Otxas, which is the type locality of *I. biscaiense*. The specimen from the cave Irutxin (NMBE 557238) displays typical character states of *zaldivarae*.

The specimens from the *bellesi*-clade (dark blue clade in Figs. 2 and 3) were collected in the caves Lezea and Lexotoa at the border of Spain and France. The caves are 1 km apart from each other and probably contiguous. This node is supported in our investigation (posterior probability of 0.97 and bootstrap value of 85 in Fig. 2, respectively, 0.94 and 80 in Fig. 3). In both phylogenetic trees (Fig. 2 and 3), the two investigated specimens have a bootstrap value of 100. The p-distance is 0.0039. From a morphological perspective, they have a similarly high-spired, conical shell form, but the aperture is clearly different. The aperture of the specimen from Lexotoa (NMBE 557234) (Fig. 5b) is oblique and has a moderately angular parietal shield. On the other hand, the parietal shield of the specimen from Lezea (NMBE 557236) (Fig. 5a) is compact and consists of thick callus, which is seemingly fused onto the body whorl. The peristome of the Lezea specimen is thick and roundish in form.

The Basque clade (Figs. 6 and 7) splits into two: a narrow, more centrally distributed *vasconicum*-clade 1 (pink clade in Figs. 2 and 3; Fig. 6) and a broader, western-reaching distribution comprising the *vasconicum*-clade 2 (light blue clade in Figs. 2 and 3; Fig. 7). The node of the split of these two clades has a low support (bootstrap value of 29 in Fig. 2, respectively 73 in Fig. 3). The split of these two clades is

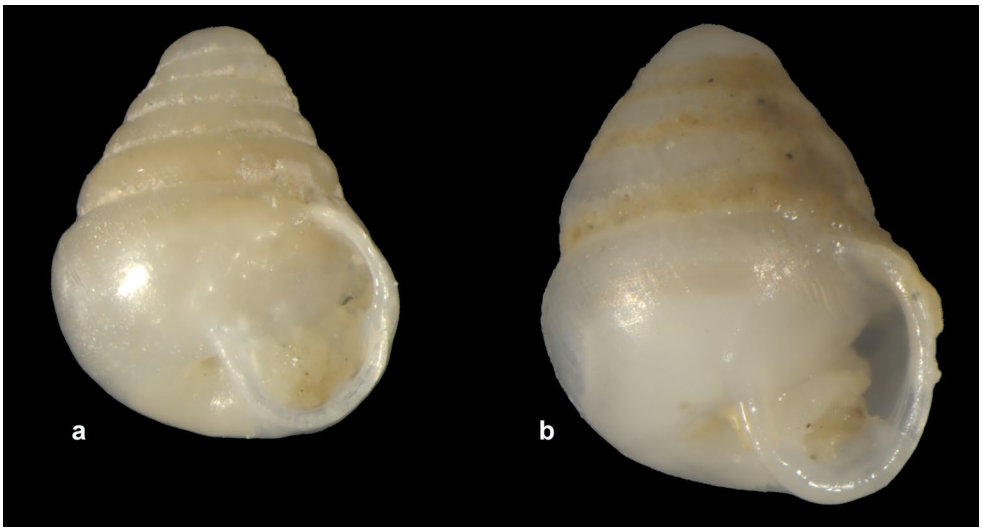

Fig. 4 Grey clade; (**a**) *Iberozospeum biscaiense* NMBE 557240, Durang, Igorre, Cueva Otxas, 23.3.2016, sh: 1.37 mm; (**b**) *Iberozospeum zaldivarae* NMBE 557238, Aralar, Arbizu, Cueva Irutxin, 20.6.2015, sh: 1.59 mm. — All phot. × 40

not supported by the Bayesian posterior probability. The topotypic specimen of *I. vasconicum* (No. 151 in Weigand et al., 2013) clusters within the pink clade. Morphologically, shells from caves clustering in the pink *vasconicum*-clade 1 (Fig. 6) showed a commensurate similarity in shell shape and apertural configuration with noticeable differences in spire height in shells from Basotxo cave (Ton de Winter, unpubl. data 2015). The two westernmost specimens NMBE 557138 and NMBE 557242 (cf. Fig. 1 and Fig. 7b, j) in the light blue *vasconicum*-clade 2 differ morphologically from the remaining *vasconicum*-like specimens in the clade.

The *vasconicum*-clade 3 (brown clade in Figs. 2 and 3) has high posterior probability and bootstrap support only in the terminal nodes. The deep nodes in the brown clade are not supported in the ML analysis (bootstrap support of 53, respectively, 57 in Fig. 3). Morphologically, they resemble typical *I. vasconicum* due to shell shape and the apertural configuration. The specimen in Fig. 8a is about 1.5 times bigger than the smallest specimen from the brown clade, but the shell shape is very similar to the other specimens in this clade. Figure 8g is remarkable due to its broad conical form, the deeply pronounced suture and the obvious, broadly deepened umbilicus. We consider it a new species.

Support values in the *schaufussi*-clade (red clade in Figs. 2 and 3) are high. In Fig. 9a, a specimen from the cave Búho, Puente Viesgo, is illustrated, which is the type locality of *I. suarezi* (Gittenberger, 1980). However, comparing our specimen with the holotype of *I.*

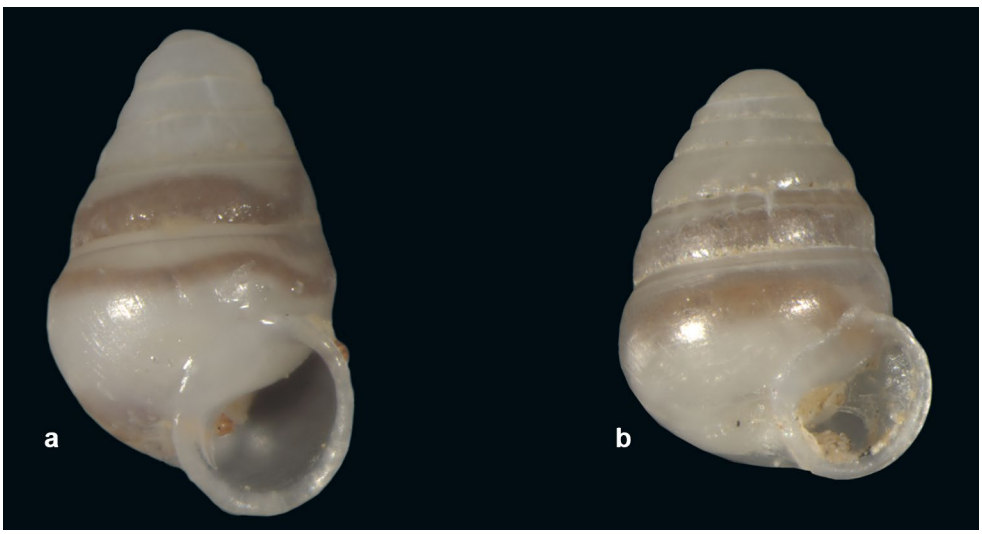

Fig. 5 *Iberozospeum bellesi.* Dark blue clade; (**a**) NMBE 557236, Zugarram, Sare, Lezea, 13.12.2015, sh: 1.67 mm. (**b**) NMBE 557234, Zugarram, Zugarramurdi, Lexotoa-2, 20.12.2015, sh: 1.38 mm. — All phot. × 40

Fig. 6 *Iberozospeum vasconicum*. Pink clade; (**a**) NMBE 557207, Aizkorri, Onati, Azkonar Zulueta, 28.5.2016, sh: 1.31 mm; (**b**) NMBE 557160, Aizkorri, Eskortatza, Urkoba, 8.3.2017, sh: 1.18 mm; (**c**) NMBE 557217, Ernio, Tolosa, Mendikute, 23.9.2017, sh: 1.5 mm; (**d**) NMBE 557219, Bust-Lea, Forua, Munarri Arrola, 9.12.2017, sh: 1.56 mm; (**e**) NMBE 557209, Aizkorri, Onati, Cueva Iritegi, 28.5.2016, sh: 1.43 mm; (**f**) NMBE 557150, Aizkorri, Onati, Txomenkoba Goikoa, 16.12.2015, sh: 1.27 mm; (**g**) NMBE 557156, Udalaitz, Elorrio, Cueva Artegi, 17.5.2016, sh: 1.48 mm; (**h**) NMBE 557168, Aizkorri, Onati, Arlaban, 11.2017, sh: 1.27 mm; (**i**) NMBE 557154, Udalaitz, Aretxabaleta, Cueva Penpelin, 26.4.2016, sh: 1.34 mm; (**j**) NMBE 557166, Aizkorri, Onati, Aizkirri, 11.2017, sh: 1.59 mm; (**k**) NMBE 557223, Durang, Igorre, Otxas, 23.3.2016, sh: 1.24 mm; (**l**) NMBE 557152, Udalaitz, Arrasate, San Valerio (Galarra), 23.3.2016, sh: 1.25 mm. No picture of NMBE 540554.4, 540555.2, 540556.1 (shell destroyed). — All phot. × 40


a
b
c
d
e
f
g
h
i
j
k
l
m
n
o
p

◂**Fig. 7** *Iberozospeum vasconicum*. Light blue clade; (**a**) NMBE 557198, Cueva de la Fuente de Estragueña, 16.6.2011, sh: 1.26 mm; (**b**) NMBE 557138, Castro, Laredo, La Baja, 12.4.2017, sh: 1.11 mm; (**c**) NMBE 557232, Triano, Galdames, Mina Princesa (superior), 3.7.2016, sh: 1.51 mm; (**d**) NMBE 557211, Triano, Güenes, Grazal, 2.10.2016, sh: 1.49 mm; (**e**) NMBE 557174, Triano, Galdames, Escachabel-2 (Urallaga), 1.4.2013, sh: 1.44 mm; (**f**) NMBE 557200, Triano, Galdames, Bitzkaia, Cueva de la San Juan, 10.6.2012, sh: 1.23 mm; (**g**) NMBE 557189, Durang, Atxondo, Azkillar (=Galtaikoba), 16.3.2014, sh: 1.19 mm; (**h**) NMBE 557182, Durang, Zeberio, Cueva Hatxondo, 30.12.2012, sh: 1.28 mm; (**i**) NMBE 557221, Aralar, Arbizu, Cueva Irutxin, 20.6.2015, sh: 1.54 mm; (**j**) NMBE 557242, Ason, Matienzo, Cueva Cubija (=Marcos), 19.7.2016, sh: 1.34 mm; (**k**) NMBE 557178, Salvada, Berberana, Las Paules, 21.6.2011, sh: 1.3 mm; (**l**) NMBE 557180, Salvada, Izarra, Torca Lejazar, 28.12.2013, sh: 1.29 mm; (**m**) NMBE 557244, Salvada, Berberana, Las Paules, 9.11.2013, sh: 1.28 mm; (**n**) NMBE 557158, Aizkorri, Eskoriatza, Saiturri-2, 22.2.2017, sh: 1.47 mm; (**o**) NMBE 557187, Aralar, Ataun, Cueva Akaitz Txiki, 14.1.2014, sh: 1.47 mm; (**p**) NMBE 557188, Aralar, Ataun, Cueva Akaitz Txiki, 14.1.2014, sh: 1.32 mm. NMBE 557162, Aizkorri, Parzoneria, Perusaroi-1, 15.5.2017 (subadult shell, not shown on plate). No pictures of NMBE 540551.1, 540552.1, 540552.3, 540553.1 (shells destroyed). — All phot. ×40

suarezi (RMNH.MOL.55383) (Jochum et al., 2019: 72, Fig. 4a–c), it is evident that this is the same species. The specimens from the two Cantabrian clades have a more elliptical aperture compared with the *vasconicum*-clade specimens (pink, light blue and brown clades in Figs. 2, 3, 6, 7, and 8).

The Asturian clade splits into two subclades (purple and green clades in Figs. 2 and 3). Support values within these clades are moderate to high. Weigand et al. (2013: Fig. 5) sequenced two specimens from the Cueva del Bosque/Cueva Inguanzo, which cluster within the purple clade (Figs. 2 and 3). Moreover, Weigand et al. (2013) identified these two specimens as *I. suarezi* and considered them "evolutionary lineage Z14" (No. 140 in Weigand et al., 2013 in our trees). Jochum et al. (2019: 83–84, Fig. 15) explained that this cave is situated 1 km opposite of the cave, Cueva del Puente de Inguanzo, which is the cave Gittenberger (1980) considered to be inhabited by *I. schaufussi* sensu Gittenberger (1980: Fig. 1) and *I. suarezi* Gittenberger (1980: Fig. 2). These two taxa were recognised by Jochum et al. (2019) to be misidentifications and were subsequently described as new species, viz., *I. gittenbergeri* Jochum (Jochum, Prieto & De Winter, 2019 in Jochum et al., 2019) and *I. praetermissum* Jochum (Jochum, Prieto & De Winter, 2019 in Jochum et al., 2019). Since *I. gittenbergeri* is known only from a single shell and no clearly definable, live adult snail was found, it could not be included in this study. In Figs. 2 and 3, a specimen from the "evolutionary lineage Z14" (Weigand et al., 2013) and another species (Fig. 10f) from Cueva del Puente Inguanzo are included. The specimen in Fig. 10f was found at the type locality of *I. praetermissum*. This specimen is a juvenile and the identification is not clear since the aperture is not fully grown. The specimens in Figs. 10a–e have a high, conical spire and a barely developed lamella on the columella (Fig. 10d) and are considered to be *I. praetermissum*. The p-distance from the specimen in Fig. 10f and the topotypic specimen No. 140 from Weigand et al. (2013) is 0.0086. The mean p-distance from the investigated specimens in the purple clade (Figs. 2 and 3, Fig. 10a–f) and the specimen, No. 140 from Weigand et al. (2013), is 0.006.

The green clade contains various morphs. The topotype specimen of *I. percostulatum* (Fig. 10h) from the cave Herrería is a juvenile. In this cave, another species, here considered to be *I. praetermissum*, (Fig. 10b) lives in syntopy or at least in sympatry with *I. percostulatum*. Another well-supported lineage is visible in Fig. 10i and j, with both specimens originating from the same population in El Toyo in Cantabria; the two shells are morphologically quite different, illustrating shell variability within the lineage. The shell of the specimen from the Picos (Fig. 10k) is broadly conical, with a remarkably narrow-stepped coiling pattern of the teleoconch whorls and a large elliptical aperture. The group comprising Fig. 10l–n, forms another lineage in the green clade, which is characterised by broad conical shells resembling the specimen from the Picos, but with high and well-rounded teleoconch whorls.

The yellow clade (Figs. 2, 3, and 11) contains ribbed specimens with varying degrees of superficial striation. Although the specimen in Fig. 11a has less-pronounced ribs, they are clearly visible in apical view. This shell bears a deep suture and its aperture is elliptical and reverted. The specimen in Fig. 11b is a juvenile but the ribs are clearly visible. Although the shell morphology is different, it clusters together with specimen 11c, with a bootstrap support of 95 (Fig. 2). The p-distance of these individuals is 0 since only the nuclear marker H3 could be sequenced for both specimens and this sequence is identical. On the other hand, the strongly ribbed specimen in Fig. 10c constitutes the new species, *Iberozospeum costulatum* n. sp.

The ABGD assigned the 45 *Iberozospeum* COI sequences into 22 groups. The Barcode gap distance is 0.012. In Table 3 are the groupings of the ABGD analysis. Since we do not have the COI sequences of all investigated animals, not all specimens could be assigned to a group. The two animals from the same population from Toyo Cave (NMBE 557225 and 557226) were divided into different groups. Using ABGD, all animals from the pink *vasconicum*-clade were classified into group 1. Group 2 consists exclusively of animals from the light blue *vasconicum*-clade. Some animals from the light blue *vasconicum*-clade were classified into other groups (Table 3). The two animals from the *schaufussi*-clade (NMBE 559628 and 559630) were placed in group 6. The specimens from the *praetermissum*-clade were placed in group 7. The two specimens from the *bellesi*-clade (NMBE 557234 and 557236) were assigned in group 15. The remaining groups each contain only one animal.

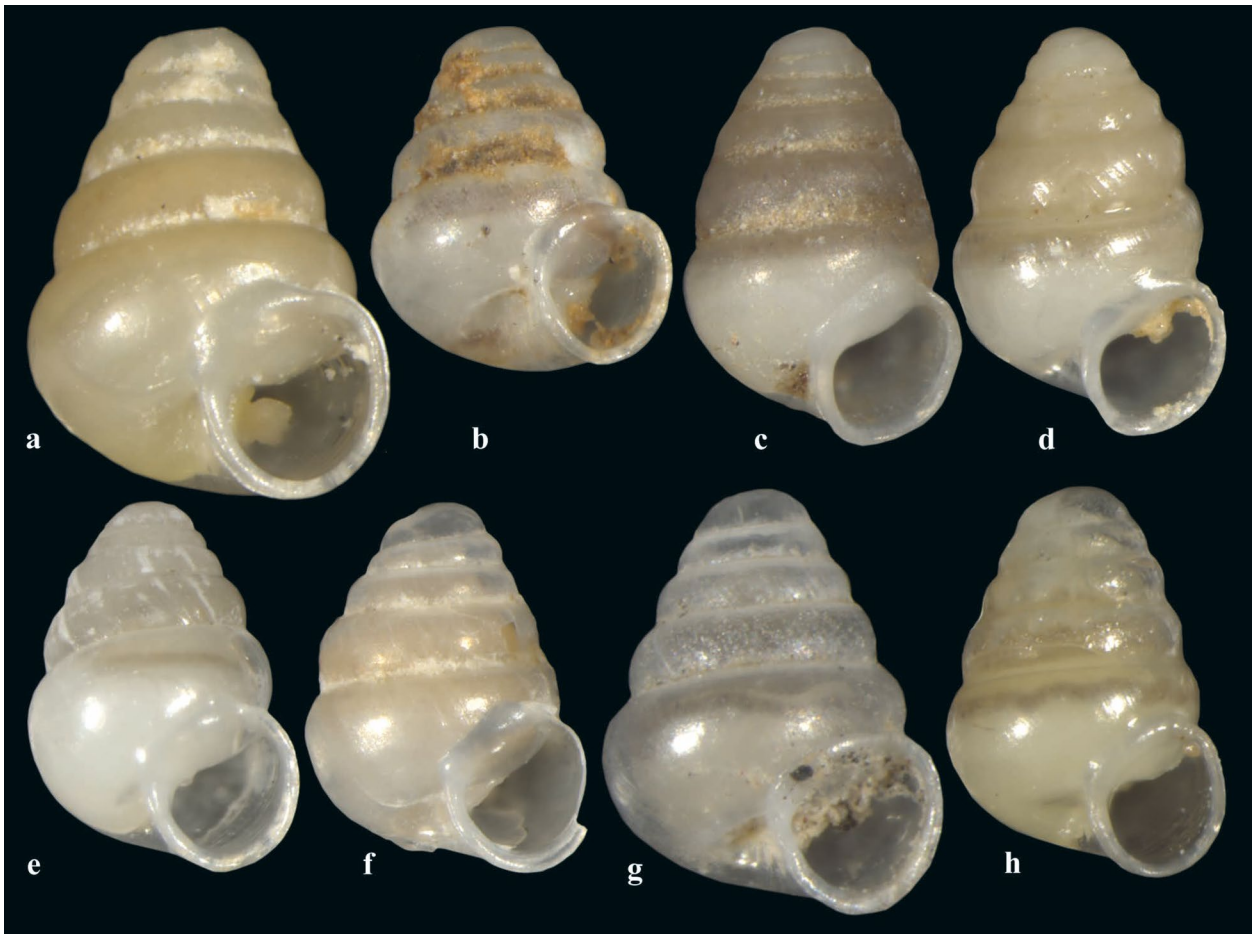

Fig. 8 *Iberozospeum vasconicum*. Brown clade; (**a**) NMBE 559634, Cantabria, Entrambasaguas, Murcielagos, 28.3.2018, sh: 1.56 mm; (**b**) NMBE 559624, Cantabria, Entrambasaguas, Iglesia, 28.3.2018, sh: 1.14 mm; (**c**) NMBE 557215, Cantabria, Santiurde de Reinosa, Las Arrigueras, 20.1.2018, sh: 1.39 mm; (**d**) NMBE 559632, ditto, 29.3.2018, sh: 1.36 mm; (**e**) NMBE 557213, Guareña, Merindad de Sotoscueva, Garcia, 26.11.2017, sh: 1.23 mm; (**f**) NMBE 557146, Miera, Soba, Las Montosas, 20.2.2016, sh: 1.23 mm; (**g**) NMBE 557229, Ason, Arredondo, San Juan de Socueva, 12.4.2017, sh: 1.41 mm; (**h**) NMBE 559636, Cantabria, Entrambasaguas, Prementera, 28.3.2018, sh: 1.3 mm. — All phot. ×40

Morphology

Although only one member of *Iberozospeum* is histologically sectioned here, sections of the upper visceral complex of topotypic *I. vasconicum* (AJC 1848) show that the anatomy follows the general carychiid design (Morton, 1955; Harry, 1997–1998) and that described for *Zospeum* in Maier (1982), Dörge (2010), and Jochum et al. (2015b) as well as in Barker (2001) for aspects of the Ellobiidae (Fig. 12). The cross-sections reveal no phylogenetic differences but rather, seasonal differences in the specific individuals. The *I. vasconicum* individual, collected in June 2011, is aphallate. Euphally was detected by Jochum et al. (2015b) in *Z. amoenum* (von Frauenfeld, 1856) (species revised from "*Zospeum* sp." in Inäbnit et al., 2019), collected in August 2008 from Konečka zijalka, Slovenia. The histological sections of the upper visceral complex of individuals of topotypic *Z. isselianum* (Pollonera, 1887) (AJC 2287) and *Z. spelaeum* (Rossmässler, 1839) (AJC 848) from the Dinarides (Fig. 12a–b) in this work also show that these snails were aphallate during time of collection in June and October, respectively. The same upper visceral region of the snail (cuts 14–22) in our histological sections (Fig. 12) shows different perspectives due to the generally larger size of the two Dinaride individuals in this study. Visible in clockwise rotation from the outside in, *Z. isselianum* shows the mantle gland (mag), the cerebral ganglion (cg), the mantle cavity (mc), the pleural ganglion (pg), the foot (f), the pharynx (ph), the oesophagus (oe), the statocyst containing otoliths and the columellar muscle (cm) (Fig. 12a). For *Z. spelaeum*, the same clockwise perspective shows the mantle gland (mag), the foot (f), some haemolymph (hl), the pharynx (ph), the oesophagus (oe), a hump shaped upper, non-vascularized columellar muscle (cm) and a moderately long genital opening (go) (Fig. 12b). For *I. vasconicum,* a remarkably huge, glandular albumen gland (ag) is clearly

visible (Fig. 12c). This is a compound, sac-like enlargement of the oviduct and is responsible for producing albumen for the formation of the eggs (Luchtel et al., 1997). The albumen gland is a female accessory sex gland, which enlarges with sexual maturation of the animal. The size of this gland is considered to determine the maximum number of eggs that can be produced at any one time (Barker, 2001). Due to the presence and large size of the albumen gland (indicative of the female phase) here, modification in existing structures and superposition of others on the fundamental carychiid pattern is clearly the case. Also, strikingly apparent is the large, well-developed, mucous gland (stained reddish violet) (mg). Additionally, visible in the clockwise perspective of the upper visceral complex of *I. vasconicum* is the kidney (k) with a prominent renopericardial passage and the heart (h) located at the base of the kidney, haemolymph (hl) at the foot section (f), the contractile pneumostome (p), the mantle gland (mag), the pharynx (ph) and oesophagus (oe), the vascularized, 2-humped columellar muscle (cm) and the long genital opening (go) (Fig. 12c). We remark that deeper analysis of anatomical aspects and individual structural analyses of *Iberozospeum* is beyond the scope of this paper and will be presented in a future work.

Significant however, for *Iberozospeum* n. gen., is that the columellar muscle shows prominent humps, which contain vasculature extending to the tips of these humps (Fig. 12c). In our investigation of the columellar lamellae of *Iberozospeum*, the dense, scaley crystallographic structure on localised zones of the lamellae correlates perfectly with the corresponding points of contact of these two hump-like elevations of the columellar muscle (Fig. 13). In sync with this observation, Barker (2001) emphasized there is a trend amongst the Ellobiidae that the columellar muscle becomes detached from the body wall from its origin on the columella and has become largely free in the haemocoel. The columellar muscle, thus, runs forward to attach on the cephalic organs and anterior body wall (Barker, 2001). In this case, rather than just simply retracting, the cephalopedal mass becomes inverted when the animal retracts into the shell (Barker, 2001). In *Iberozospeum*, the columellar muscle is indeed detached except at these two points of contact. In the Alpine and Dinaride species of *Zospeum*, crystallographic structure is not overlapping and not restricted to specific points. Moreover, it is comprised of low shoals of crystallographic structure (seen also in fossil Carychiidae in Jochum et al., 2015c, Fig. 5), randomly interspersed over the columellar lamellae deep in the shells of *Z. spelaeum* from two separate caves in Slovenia (MCBI CSR SASA 37049a, Velika Pasica and AJC 847, Betalov Spodmol Grotte) (Fig. 13a–b) here. Remarkable are the dense, localised, overlapping wedges of crystallographic structure on the complementary points of the columellar lamellae in the empty shells of the Iberian taxa: *Iberozospeum* sp. RMNH.MOL.234120 (Cueva Refugio, Trucios) (Fig. 13c–d), on the upper part of the lamella of *Iberozospeum* sp. RMNH.MOL.234104 (Cueva del Comediante) and on the lamella of *Iberozospeum* sp. RMNH.MOL.234141 (Cueva a Sul, Oviedo) (Fig. 13e–f) as well as on that of *I. vasconicum* (AJC 1849, Cueva Arrikrutz) (Fig. 13g–h). The lower lamella of *I.* sp. RMNH.MOL.234120 (Cueva Refugio, Trucios) clearly shows the specific locality of the contact point of the columellar muscle (Fig. 13c–d). Shells of RMNH.MOL.234104 (Cueva del Comediante) and RMNH.MOL.234141 (Cueva a Sul, Oviedo) (Fig. 13e–f), which were initially preserved in 75% ethanol, still show the characteristic, rough crystallographic structure despite deterioration by the ethyl-alcohol treatment subjected to them by the collector (Notenboom & Meijers, 1985).

Our morphological investigations also included the radulae of four Dinaride and eastern Alpine taxa described and imaged in Inäbnit et al. (2019, Supplementary Figs. S17–21) including *Z. exiguum* (Kuščer, 1932) (NMBE 553384) (Inäbnit et al., 2019, Fig. S17a–d); *Z. obesum* (von Frauenfeld, 1854) (NMBE 553409) (Inäbnit et al., 2019, Fig. S18f–h); *Z. pretneri* (Bole, 1960) (NMBE 553290) Inäbnit et al., 2019, Fig. S19a–d); and *Z. spelaeum* (Rossmässler, 1839) (NMBE 553311) (Inäbnit et al., 2019, Fig. S20e–f). These were compared with radulae extracted from individuals collected from the westernmost-sampled caves by Oviedo (Asturias) and radulae from topotypic material of *Z. vasconicum* (Prieto et al., 2015 in Jochum et al., 2015a) (AJC 1847) and *Z. zaldivarae* (Prieto et al., 2015 in Jochum et al., 2015a) (AJC 1876).

In this comparative study, the narrow radular ribbons of Dinaride *Zospeum* are tapered to an obtuse or to a straight base as in *Z. exiguum* (Fig. 14a) or a straight base as in *Z. pretneri* (Fig. 14b). The Iberian radulae have a tapered

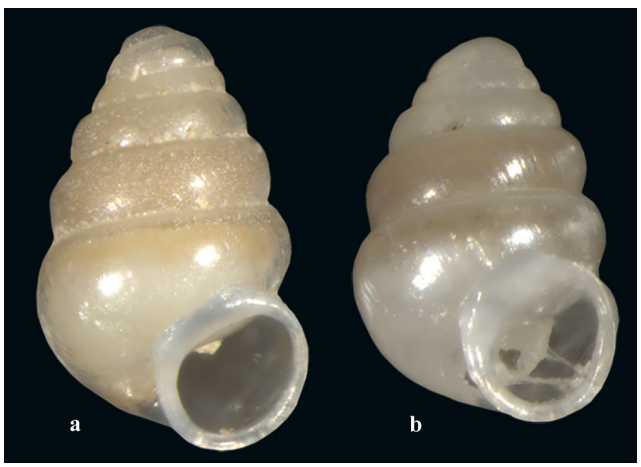

Fig. 9 *Iberozospeum schaufussi*. Red clade; (**a**) NMBE 559630, Cantabria, Puente Viesgo, Búho, 27.3.2018, sh: 1.41 mm; (**b**) NMBE 559628, Cantabria, Puente Viesgo, Soldados, 27.3.2018, sh: 1.28 mm. — All phot. × 40


a
b
c
d
e
f
g
h
i
j
k
l
m
n

◂**Fig. 10** *Iberozospeum praetermissum*. Purple clade; a–f. (**a**) NMBE 557144, Cantabria, Cabezon-MS, Udias, Udias (Cobijon), 28.8.2016, sh: 1.25 mm; (**b**) NMBE 557253, Asturias, Llanes, Cueva La Herrería, 23.12.2017, sh: 1.34 mm; (**c**) NMBE 557255, Leon, Soto de Sajambre, Cueva Busecu, 10.3.2018, sh: 1.37 mm; (**d**) NMBE 557246, Asturias, Candamo, Cueva de la Peñona de Valdemora, 5.3.2018, sh: 1.22 mm; (**e**) NMBE 557140, Asturias, Llanes, Collubina, 18.7.2017, sh: 1.35 mm; (**f**) NMBE 559620, Cantabria, Cueva Puente Inguanzo, 6.4.2018, sh: 1.29 mm. — *Iberozospeum* spp. Green clade; g–n. (**g**) NMBE 559622, Cantabria, Cueva La Zurra, 6.4.2018, sh: 1.31 mm; (**h**) NMBE 557136, Asturias, Llanes, La Herrería, 18.7.2017, sh: 1.14 mm; (**i**) NMBE 557226, Cantabria, Lamason, El Toyo, 11.7.2015, sh: 1.7 mm; (**j**) NMBE 557225, Cantabria, Lamason, El Toyo, 11.7.2015, sh: 1.33 mm; (**k**) NMBE 557142, Asturias, Picos, Cabrales, Torca Cumbre, .8.2016, sh: 1.45 mm; (**l**) NMBE 557251, Asturias, Parres, Cueva El Caleru, 10.3.2018, sh: 1.41 mm; (**m**) NMBE 557249, Asturias, Yernes y Tameza, Cueva Llagar, 2.2.2018, sh: 1.49 mm; (**n**) NMBE 557247, Asturias, Candamo, Cueva de la Peñona de Valdemora, 5.3.2018, sh: 1.48 mm. — All phot. ×40

anterior end (velum), followed by a well-defined adhesive zone leading to a remarkably straight, carpet-like swath of longitudinal rows of smaller teeth and more of them per transverse row (Figs. 14c–h, 15c). The rachidian and lateral teeth of *I. vasconicum* demonstrate remarkable similarity to those of *Carychium ibazoricum* Bank & Gittenberger, 1985, imaged in Martins (2007, Fig. 138) (Fig. 15e). The rachidian and lateral teeth of the radula of topotypic *I. vasconicum* (AJC 1848) show long endo- and ectocones flanking the mesocone by one half–three fourths the length of the mesocone (Fig. 15e). The radula of topotypic *Z. pretneri* (NMBE 553290), *I. vasconicum*'s externally most similar phenotypic relative from the Dinarides, shows endo- and ectocones that are one third–one half the length of the mesocone (Fig. 15a). Medial grooves are visible on the mesocones of *Z. pretneri* and *Z. isselianum* (AJC 874, Turjeva jama, Sovenia) here (Fig. 15a–b) as well as in a number of other eastern Alpine and Dinaride species (see Inäbnit et al., 2019, Supplementary Figs. S17–21). The basal plates are generally more compact and shorter in the radulae of Iberian taxa (Figs. 15c–e, h) versus the longer and thinner versions of those of the eastern Alpine and Dinaride *Zospeum* species (Fig. 15a–b) (see also Inäbnit et al., 2019, Supplementary Figs. S17–21). Basal plates maintain the spacing of teeth and support them in the feeding process (Luchtel et al., 1997). The radular ribbon of topotypic *I. zaldivarae* (AJC 1876) shows a rachidian tooth with a long pointed mesocone and very short endo- and ectocones that are about one fourth the length of the mesocone (Fig. 15g). The lateral teeth bear very short mesocones flanked by long, fang-like endo- and

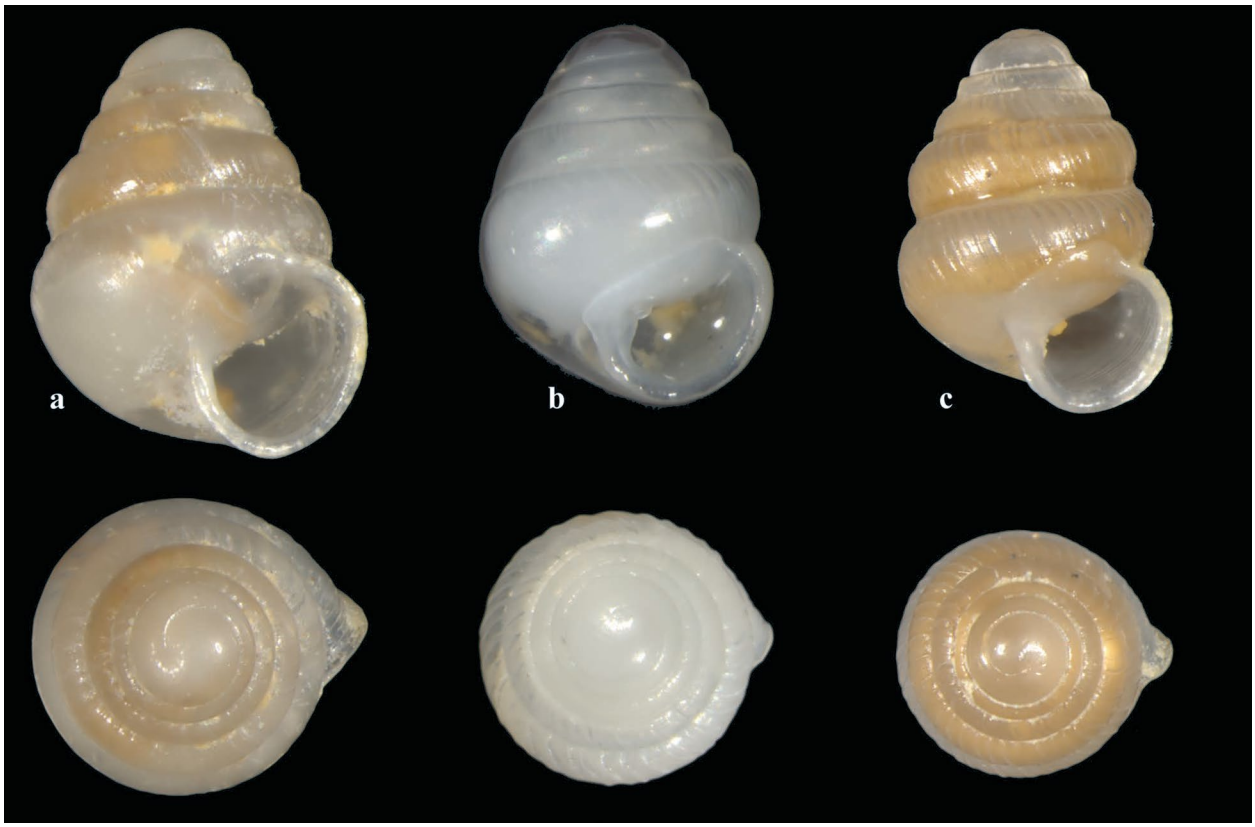

Fig. 11 *Iberozospeum costulatum*. Yellow clade; (**a**) NMBE 559626, Cantabria, Lierganes, Cesareo, 21.3.2016, sh: 1.42 mm; (**b**) NMBE 557227, Cantabria, Ason, Soba, Cuvias Negras, 12.4.2017, sh: 1.27 mm; (**c**) NMBE 557231, Alen, Sopuerta, Valdebeci, 20.10.2015, sh: 1.27 mm. — All phot. ×40

Table 3 Results of the species delimitation method ABGD

NMBE-No	ZUPV-No	Cave and Province	ABGD group	clade
557150	3405	Txomenkoba (Gipuzkoa)	1	*vasconicum* (pink)
557152	3758	San Valerio (Gipuzkoa)	1	*vasconicum* (pink)
557154	3849	Penpelin (Gipuzkoa)	1	*vasconicum* (pink)
557156	3856	Artegi (Bizkaia)	1	*vasconicum* (pink)
557166	4990	Aizkirri (Gipuzkoa)	1	*vasconicum* (pink)
557168	5005	Arlaban (Gipuzkoa)	1	*vasconicum* (pink)
557209	3904	Iritegi (Gipuzkoa)	1	*vasconicum* (pink)
557217	4930	Mendikute (Gipuzkoa)	1	*vasconicum* (pink)
557219	5087	Munarri Arrola (Bizkaia)	1	*vasconicum* (pink)
557223	3728	Otxas (Bizkaia)	1	*vasconicum* (pink)
540551_1	1847	Akaitz Txiki (Gipuzkoa)	2	*vasconicum* (light blue)
540552_1	2039	Azkillar (Bizkaia)	2	*vasconicum* (light blue)
540552_3	2039	Azkillar (Bizkaia)	2	*vasconicum* (light blue)
557178	1607	Paules (Burgos)	2	*vasconicum* (light blue)
557187	1847	Akaitz Txiki (Gipuzkoa)	2	*vasconicum* (light blue)
557188	1847	Akaitz Txiki (Gipuzkoa)	2	*vasconicum* (light blue)
559632	5213	Arrigueras (Cantabria)	3	*vasconicum* (brown)
557189	2039	Azkillar (Bizkaia)	4	*vasconicum* (light blue)
557138	4702	Baja (Cantabria)	5	*vasconicum* (light blue)
559628	5175	Soldados (Cantabria)	6	*schaufussi* (red)
559630	5171	Buho (Cantabria)	6	*schaufussi* (red)
557140	4862	Collubina (Asturias)	7	*praetermissum* (purple)
557246	5210	Valdemora (Asturias)	7	*praetermissum* (purple)
557253	5209	Herreria (Asturias)	7	*praetermissum* (purple)
557255	5208	Busecu (Leon)	7	*praetermissum* (purple)
559620	5257	Puente Inguanzo (Asturias)	7	*praetermissum* (purple)
557249	4915	Llagar (Asturias)	8	spp. (green)
557251	5211	Caleru (Asturias)	8	spp. (green)
559626	3807	Cesareo (Cantabria)	9	*costulatum* (yellow)
557242	4057	Cubija (Cantabria)	10	*vasconicum* (light blue)
557213	5006	Garcia (Burgos)	11	*vasconicum* (brown)
557200	854	San Juan-9 (Bizkaia)	12	*vasconicum* (light blue)
557211	4864	Grazal (Bizkaia)	12	*vasconicum* (light blue)
559624	5203	Iglesia (Cantabria)	13	*vasconicum* (brown)
559634	5200	Murcielagos (Cantabria)	13	*vasconicum* (brown)
557238	2875	Irutxin (Navarra)	14	*biscaiense* (grey)
557234	3371	Lexotoa-2 (Navarra)	15	*bellesi* (dark blue)
557236	3323	Lezea (Navarra)	15	*bellesi* (dark blue)
557146	3820	Montosas (Cantabria)	16	*vasconicum* (brown)
557232	4017	Princesa (Bizkaia)	17	*vasconicum* (light blue)
557158	4601	Saiturri-2 (Gipuzkoa)	18	*vasconicum* (light blue)
557225	4102	Toyo (Cantabria)	19	spp. (green)
557226	4102	Toyo (Cantabria)	20	spp. (green)
557144	4136	Udias (Cantabria)	21	*praetermissum* (purple)
559622	5258	Zurra (Asturias)	22	spp. (green)

ectocones on compact basal plates. The size and shape of teeth vary from row to row (Fig. 15h). As it is known for many ellobiids, the transition from the lateral teeth to the pectinate marginal teeth is abrupt (Fig. 15e) or gradual via a few intermediate, transitional teeth (Fig. 15c, h) (Martins, 1996, 2007). Within the central longitudinal rows of the radulae, the rachidian teeth of the individuals from Asturias (Fig. 15c–d) and Burgos (Fig. 15f) show a long mesocone

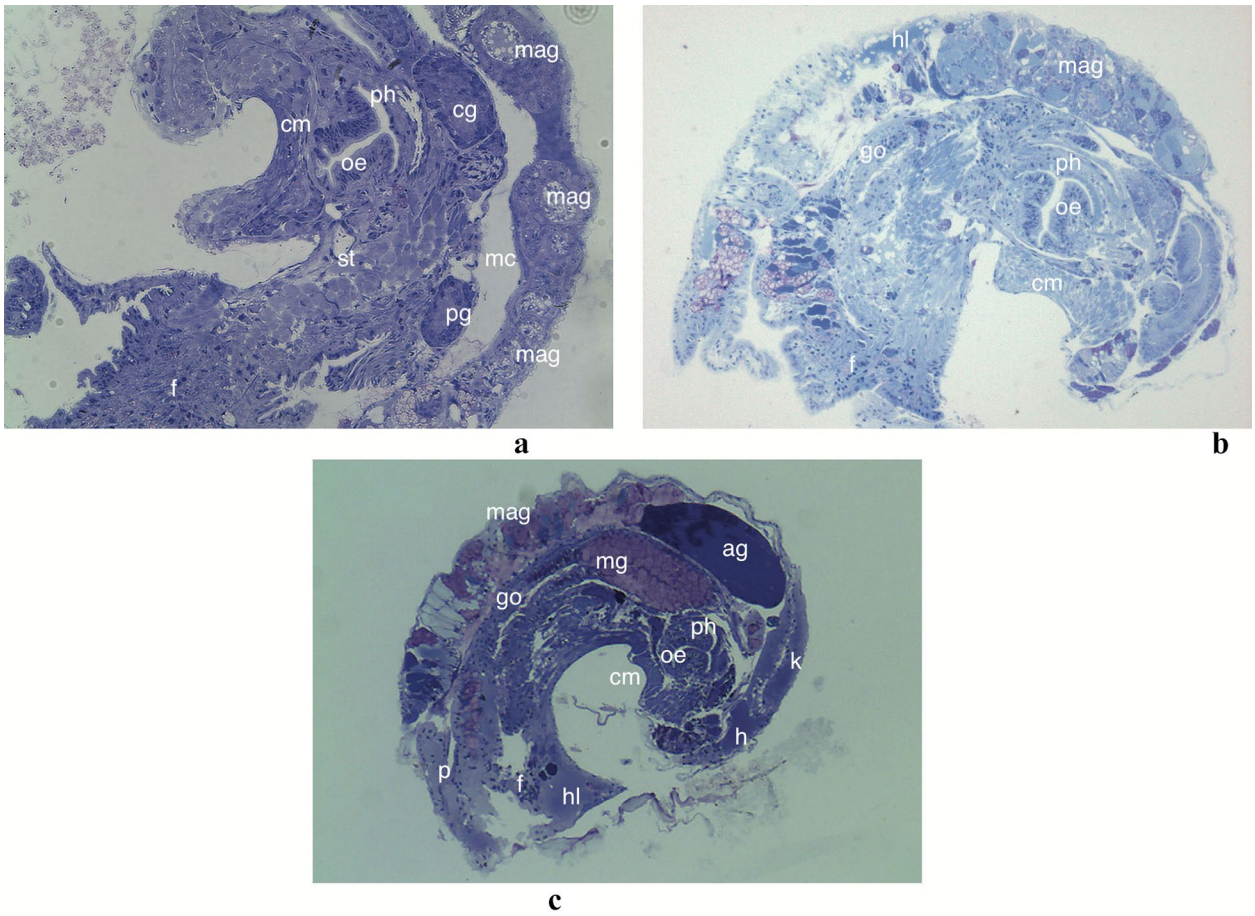

Fig. 12 Light micrograph showing histological overview of the upper visceral mass of *Zospeum* and *Iberozospeum.* Visible structures vary due to the season of collection, degree of sexual maturity of the individual and the presence of certain structures and the superposition of others. Labels proceed clockwise rotating from the outside in; (**a**) topotypic *Z. isselianum* (AJC 2287), Turjeva jama, Slovenia (46.2435, 13.5046): mantle gland (mag), foot (f), mantle cavity (mc), cerebral ganglion (cg), pleural ganglion (pg), pharynx (ph), oesophagus (oe), statocyst (st), pedal ganglion (pg), columellar muscle (cm); (**b**) *Z. spelaeum* (AJC 848), Betalov Spodmol jama, Slovenia (45.7922, 14.1877): mantle gland (mag), foot (f), genital opening (go), pharynx (ph), oesophagus (oe), statocyst (st), columellar muscle (cm); (**c**) topotypic *I. vasconicum* (AJC 1848), Cueva de la Ermita de Sandaili, Spain (42.9994, -2.4381): mantle gland (mag), giant albumen gland (ag), kidney with renopericardial passage (k), heart (h), foot with haemolymph (f, hl), long genital opening (go), large mucus gland (mg), pharynx (ph), oesophagus (oe), two humps of vascularised columellar muscle (cm). scale: 500 µm. — All images taken by Dorian Dörge, Goethe University Frankfurt am Main

flanked by endo- and ectocones of varying lengths from short to long. A hint of a median groove is present on some of the lopsided transitional teeth of *I. zaldivarae* (AJC 1876) (Fig. 15h). In the transverse rows, there is an increased incidence of bi-cuspid, fang-like lateral teeth (i.e. RMNH.MOL. 234,116, Cueva a Sul, Oviedo) flanking both sides of the rachidian tooth (Figs. 15c–d). As is considered for pulmonates (Luchtel et al., 1997), the teeth show constant form in the longitudinal rows but vary considerably in the transverse direction on the radular ribbon.

Individuals of *I. vasconicum* are generally smaller (Jochum et al., 2015a) than the Alpine and Dinaride species of *Zospeum*, except those comprising the *Z. pretneri* clade, which are about the same size and sometimes slightly larger (Inäbnit et al., 2019).

Discussion

In the molecular assessment, the topology generally did not change in the concatenated tree with all investigated specimens (Fig. 2) nor in the concatenated tree with complete marker sets (Fig. 3). In the latter, the support values are slightly higher and corroborate our interpretation of the phylogenetic and morphological findings. In order to understand the morphological traits in *Iberozospeum* n. gen., a figure is added here showing the type specimens of all hitherto described species (Fig. 16).

The *biscaiense-zaldivarae*-clade (grey clade in Figs. 2 and 3) contains sequences of two specimens (No. 162 and 163) from Weigand et al. (2013), who identified these

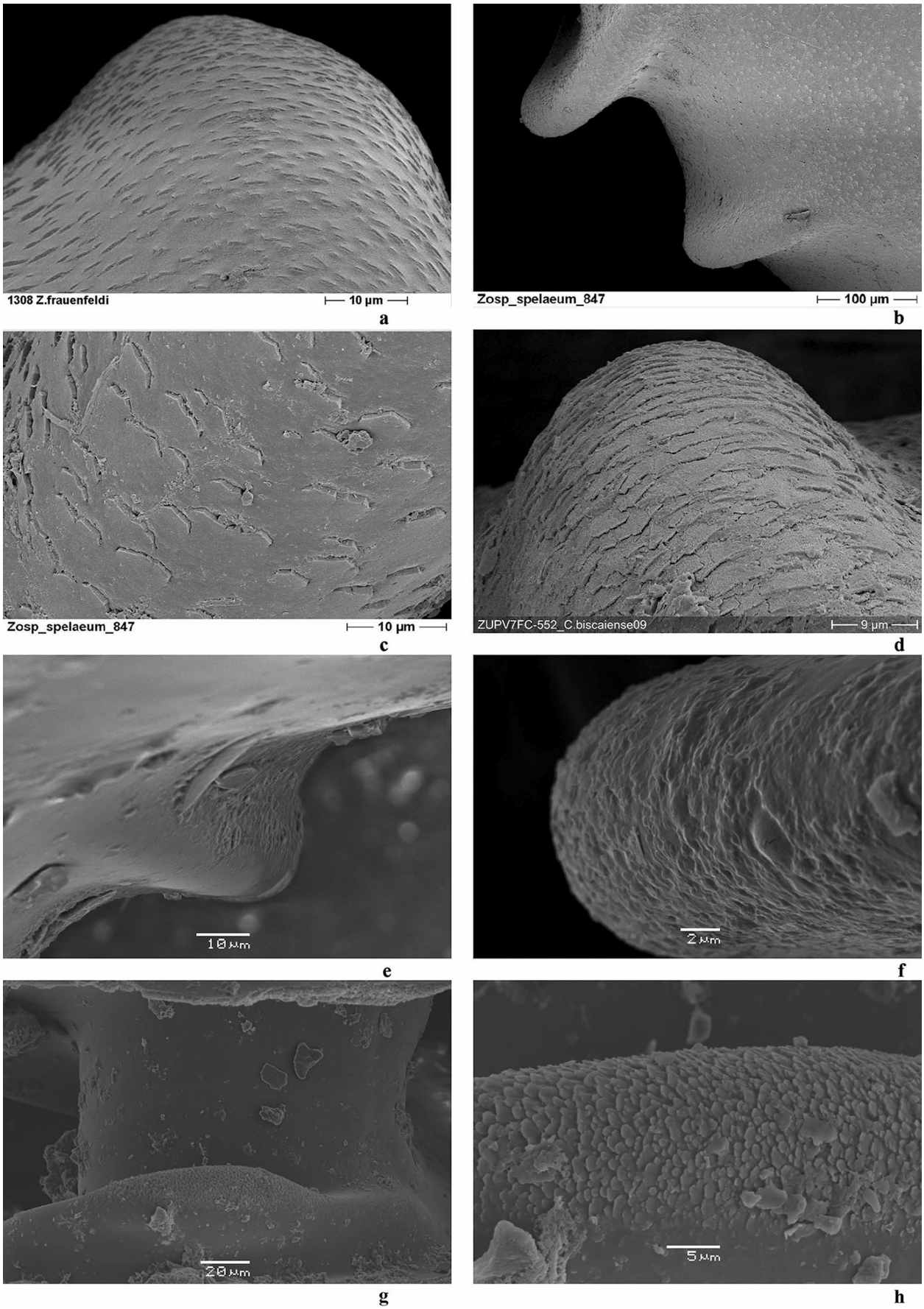
1308 Z.frauenfeldi
10 µm
a
Zosp_spelaeum_847
100 µm
b
Zosp_spelaeum_847
10 µm
c
ZUPV7FC-552_C.biscaiense09
9 µm
d
10µm
e
2µm
f
20µm
g
5µm
h

◂**Fig. 13** Crystallographic structure on the columellar lamellae of Dinaride *Zospeum* and *Iberozospeum* shells; (**a**) *Zospeum spelaeum*, (AJC 847), Betalov Spodmol jama, Slovenia (45.7922 14.1877), pattern of low, non-overlapping, wedges of crystallographic structure on the lamella; (**b**) *Zospeum spelaeum*, (MCBI CSR SASA 37049a), Velika Pasica, Slovenia (N45.9189 E14.4934), non-overlapping wedges of crystallographic structure on lamella in old shell; (**c**) *Iberozospeum* sp., (RMNH.MOL. 234,120), Cueva Refugio, Trucios, overview of dense, overlapping, scale-like wedges of localized, crystallographic structure on upper part of the lower lamella; (**d**) ibid., closeup view of c; (**e**) *Iberozospeum* sp., (RMNH.MOL. 234,104), Cueva del Comediante, Santander, upper part of the lamella of chemically treated shell showing dense, overlapping wedges of localized, crystallographic structure; (**f**) *Iberozospeum* sp., (RMNH. MOL. 234,141), Cueva a Sul, Oviedo, localized, overlapping wedges of crystallographic structure on lamella of chemically treated shell; (**g**) *Iberozospeum vasconicum*, (AJC 1849), Cueva Arrikrutz, overview of dense, localized, crystallographic structure on lower part of the lamella; h, ibid., closeup view of g. — Magnification varies for each perspective, see scale bars; Figs. a–b, g–h) imaged by M. Ruppel, (ret.) Goethe University Frankfurt am Main; Figs. c–f imaged by Dirk Vendermarel, Naturalis Biodiversity Center

specimens as lineage Z18. In 2015, Jochum et al. described the lineage Z18 as *I. zaldivarae*. The sequences of the two specimens of *I. zaldivarae* (Weigand et al., 2013) cluster with one specimen from the cave Irutxin. The cave, Otxas, is the type locality of *I. biscaiense* (Gomez & Prieto, 1983). We consider both species and supported entities; morphologically, the species differ by the mode of shell coiling (tighter in *I. biscaiense* when compared with *I. zaldivarae*) and presence of a small palatal denticle in *I. biscaiense,* which is lacking in *I. zaldivarae*.

The *bellesi*-clade (dark blue clade in Fig. 2) is not supported, although the complete marker set for both investigated specimens could be sequenced (dark blue clade in Fig. 3). A possible explanation for this finding is that *I. bellesi* belongs to a young radiation. The species is morphologically separated from the other known species in the Pyrenees, but our selected genetic markers cannot reveal the genetic differentiation of the species. The known distribution of *I. bellesi* spans the western Pyrenean region, including the French Basque Country and the Navarrese Pyrenees with the Sare-Zugarramurdi massif constituting an isolated enclave (Prieto & Zuazu, 2018). While *I. bellesi* is a unique Pyrenean species, all other known *Iberozospeum* taxa derive from the Basque-Cantabrian Mountains. Genetically, *I. bellesi* is clearly separated from the *biscaiense-zaldivarae*-clade but close to the other known species in Spain. Maybe other genetic markers are needed to reveal the genetic differentiation of *I. bellesi* from the other known species in Spain.

Within the Basque clades (pink and light blue clades in Figs. 2 and 3), the bootstrap support values and Bayesian posterior probabilities are low. This could be due to some missing markers in the concatenated tree (Fig. 2), because in the maximum likelihood tree, with complete marker sets (Fig. 3), the support values in the pink and light blue clades are much higher. The pink clade forms a polytomy with low support values. A possible explanation for this finding could be that these individuals form a young radiation. The selected genetic markers used in this study could not reveal the genetic differentiation of the specimens. The individuals in the light blue clade are genetically more differentiated than in the pink clade, but, bootstrap support values are also low. We included two specimens, NMBE 557178 and NMBE 557244 (Fig. 7k and m), which syntopically inhabit Las Paúles cave with *I. zaldivarae*. Both specimens cluster within the *vasconicum*-clade 2 (light blue clade in Fig. 2 and 3). On the morphological front, they resemble individuals in Fig. 7b and j.

The brown clade is the sister clade to the two *vasconicum*-clades (pink and light blue in Figs. 2 and 3) with high support (posterior probability of 1 and bootstrap value of 86 in Fig. 3). The support values in the deep nodes are low, maybe due to missing mitochondrial markers for some specimens. Due to genetic and morphological similarities to the *vasconicum*-clades 1 and 2 (Figs. 2, 3, 6, and 7), the specimens in the brown clade are considered to be *I. vasconicum*. We remain conservative with this clade because the subclades are not well supported. However, the type population of *I. vasconicum* (Weigand et al., 2013) is included in the pink subclade. For this reason, we consider all three subclades as *I. vasconicum*. Additional molecular methods like Next Generation Sequencing (NGS) are needed to resolve this group properly.

The *schaufussi*-clade (red clade in Figs. 2 and 3) contains a specimen from Cueva del Buho, which is the type locality for *I. suarezi* (Gittenberger, 1980). The investigated specimens from the red clade have an elongate-conical shell, moderately tightly coiled whorls and a roundish-lunate aperture typical for *I. schaufussi* (Jochum et al., 2019).

The purple clade (Figs. 2 and 3) contains the specimen No. 140 from Weigand et al. (2013), which was described by Jochum et al. (2019) as *I. praetermissum*. Morphologically, the individuals in the purple clade (Fig. 10a–f) show a uniform shell shape, except the specimen in Fig. 10f, which is a juvenile. The individual in Fig. 10d contains a clearly visible parietal tooth, which is typical for *I. praetermissum* and differentiates this species from *I. gittenbergeri* (Jochum et al., 2019). The individual in Fig. 10f cannot be clearly assigned to a species since the aperture is not fully grown. We remark, however, that this individual was found at the type locality of *I. praetermissum* (Jochum et al., 2019). The genetic analyses revealed that it clearly belongs to the *praetermissum*-clade even if its morphology is not typical for *I. praetermissum*, leading us to suggest that a certain spectrum of morphological variability within *I. praetermissum* is the case.

The lineages within the green clade (Figs. 2 and 3) have moderate to high support values but differ morphologically. Each lineage is represented by a different morph. The

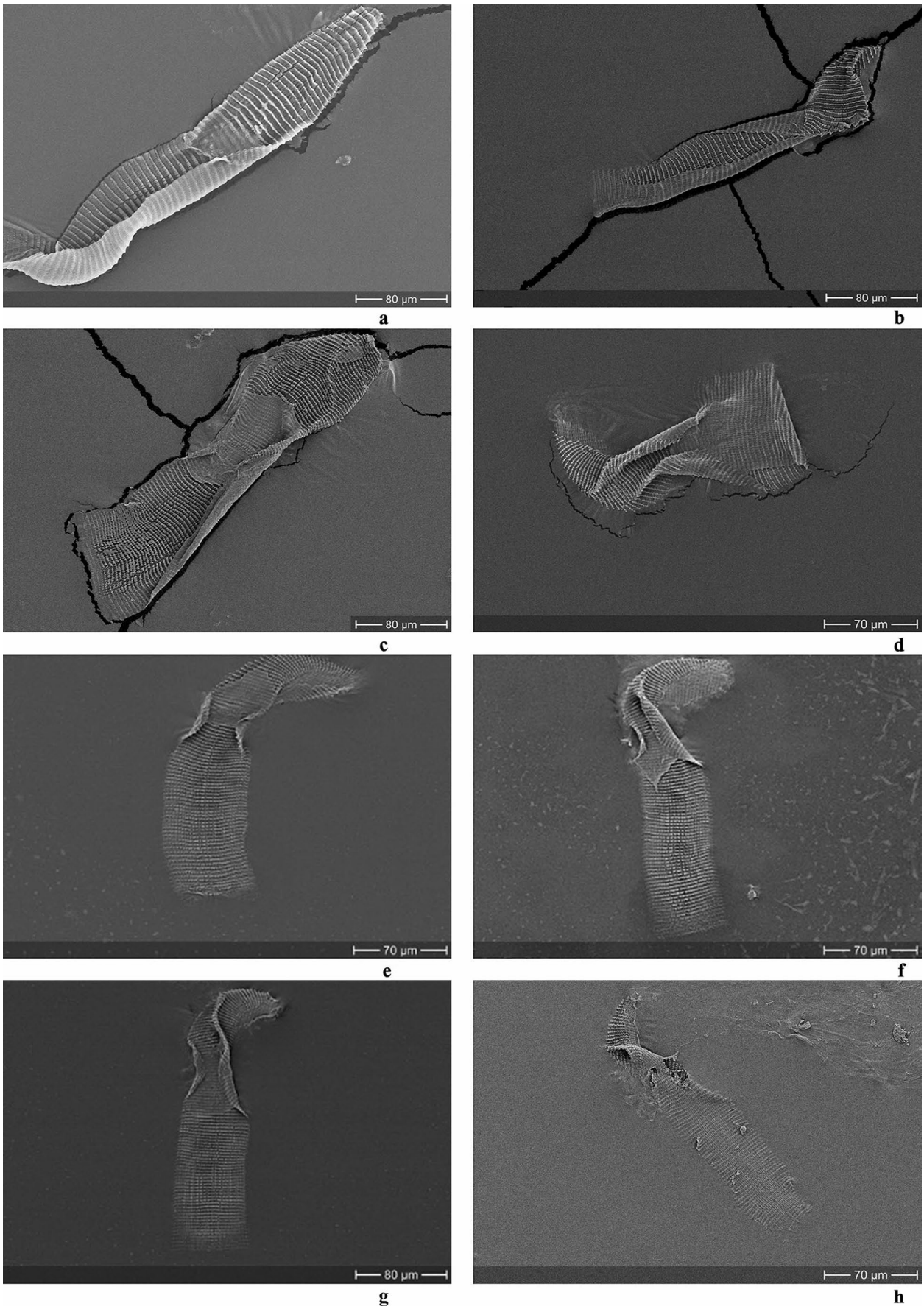
80 µm
a
80 µm
b
80 µm
c
70 µm
d
70 µm
e
70 µm
f
80 µm
g
70 µm
h

◂**Fig. 14** Scanning electron micrographs (SEM) showing radular ribbon form, middle adhesive zone (az) and rows of dentition (rd) of Dinaride and Iberian individuals (notation denotes aspects on one Dinaride *Zospeum* and one *Iberozospeum* ribbon); (**a**) *Z. exiguum* (NMBE 553384), Križna jama, Slovenia (45.7452, 14.4673), long and narrow, tapered anterior end (tae), short adhesive zone (az), bottom furled with narrow obtuse or straight base (nosb); (**b**) *Z. pretneri*, (NMBE 553290), Gornja Cerovačka pećina, Croatia (44.2701, 15.8855), ibid., with straight base; (**c**) *I. vasconicum*, (AJC 1848), Cueva Ermita de Sandaili (42.9994, -2.4381), moderately long and broad, tapered anterior end (tae), prominent adhesive zone (az), straight base (sb); (**d**) *I. zaldivarae*, (AJC 1876), Cueva de Las Paúles (43.1282, -2.7362), ibid.; (**e**) *Iberozospeum* sp. (RMNH.MOL. 234,109), Cueva de la Foz, long and broad, ibid; (**f**) *Iberozospeum* sp., (RMNH.MOL. 234,144), Cueva de Rales, very long and broad, ibid; (**g**) *Iberozospeum* sp., (RMNH.MOL. 234,116), Cueva a Sul, long and broad, ibid; (**h**) *Iberozospeum* sp., (RMNH.MOL. 234,108), Cueva de Torcona, very long and broad, ibid. — Magnification varies for each perspective, see scale bars; all Figs imaged by M. Ruppel, (ret.) Goethe University Frankfurt am Main

individual in Fig. 10h is considered to be *I. percostulatum* since it was collected at the type locality in Herrería cave and has strongly developed ribs on the teleoconch whorls, the namesake character typical for *I. percostulatum* (Alonso et al., 2018). Although it clusters together with the individual in Fig. 10g, a specimen from Cueva la Zurra, Cantabria, the specimen in Fig. 10g is considered a new species, i.e. *Iberozospeum* sp.1. It differs from the remaining specimens in the green clade due to the five loosely coiled convex whorls of the spire, an apparent parietal and basal angularity of the thick peristome, the presence of a very low parietal denticle (or thickening) in the lowermost region of the parietal part of the peristome and by the presence of a tiny denticle at the base of the columella. The specimens from El Toyo are considered a new species because they have a characteristically high, narrowly tapering, tightly coiled spire in conjunction with a thickly callused, rounded peristome fused onto the body whorl. It is not possible to recognise any dentition in the aperture in these full-bodied specimens. This combination of characters is not seen in other known Spanish taxa; therefore they are considered as *Iberozospeum* sp.2. The shells of the individuals in Fig. 10k–n resemble that of *I. gittenbergeri* by their relatively large, broad conical shape, their bearing 5.5 regularly coiled whorls and the typical, straight, long angular, thick parietal callus of the peristome (Jochum et al., 2019). The newly discovered species *Iberozospeum* sp.1 and *Iberozospeum* sp.2 are described in separate publications. The species delimitation method (ABGD) (Table 3) yielded four genetically different groups, a finding, which is not fully supported from the shell morphology. Probably, we deal here with a species complex with several cryptic species present.

The yellow clade (Figs. 2 and 3) is genetically clearly separated from the remaining clades, albeit that the complete marker set could be sequenced in only one specimen (Table 1 and Fig. 3). Morphologically, the three investigated individuals are completely different compared with the other known taxa in Spain. The specimen in Fig. 11b is a juvenile but resembles the specimen in Fig. 11c. Both specimens contain strong ribs. A new, ribbed species is described from this clade.

The caves of northern Spain show a high incidence of multiple species sympatry in contrast to those reported for the eastern Alpine and Dinaride regions (Inäbnit et al., 2019). In context, we remark here that Inäbnit et al.'s (2019) molecular investigation showed little congruency with Bole's (1974) earlier morphological interpretation of the eastern Alpine and Dinaride taxa, revealing that the incidence of multiple sympatric species is the exception, and not the rule in Dinaride caves. In Table 4, all investigated sympatric *Iberozospeum* species are listed.

The radulae of Iberian taxa show significant differences in radular ribbon form and dental morphology from those of eastern Alpine and Dinaride *Zospeum*. These differences reflect both odontophore and ribbon constitution in how it flattens out on the dorsal and lateral sections of the muscular odontophore. The ellobiid radula changes with age, with the very young specimens usually showing strongly denticulate crowns (Martins, 2007). Inäbnit et al. (2019) described four ribbon morphologies in eastern Alpine and Dinaride taxa, including those with an attenuated triangular base (*Z. isselianum, Z. frauenfeldii*) and those tapered to an obtuse to straight base as in *Z. exiguum* (Fig. 14a) or a straight base as in *Z. pretneri* (Fig. 14b) here. The form and composition of radular teeth vary according to their position on the radular membrane (referred in prepared SEM form here as ribbon) as well as diet, mineral composition of the environment, temperature and other factors (Luchtel et al., 1997). Within the ellobiids, Martins (1996, 2007) considered radular morphology a useful, distinguishing character at the generic level. For *Iberozospeum* here, the radular ribbons are clearly distinguishable from those of the Dinaride taxa. They are long and broad in form and very straight below the zone of the adhesive layer. They also bear more and smaller teeth per transverse row (Fig. 14c–h). Like those in their eastern Alpine and Dinaride relatives, they have a tapered anterior end (velum) above the adhesive layer. However, while the narrower ribbons of the latter taxa are tapered and sometimes straight at the base (i.e. *Z. pretneri*), all those of *Iberozospeum* are so far completely straight at the base, showing a flatter surface area aligned with very straight rows of teeth. We emphasize that this situation is

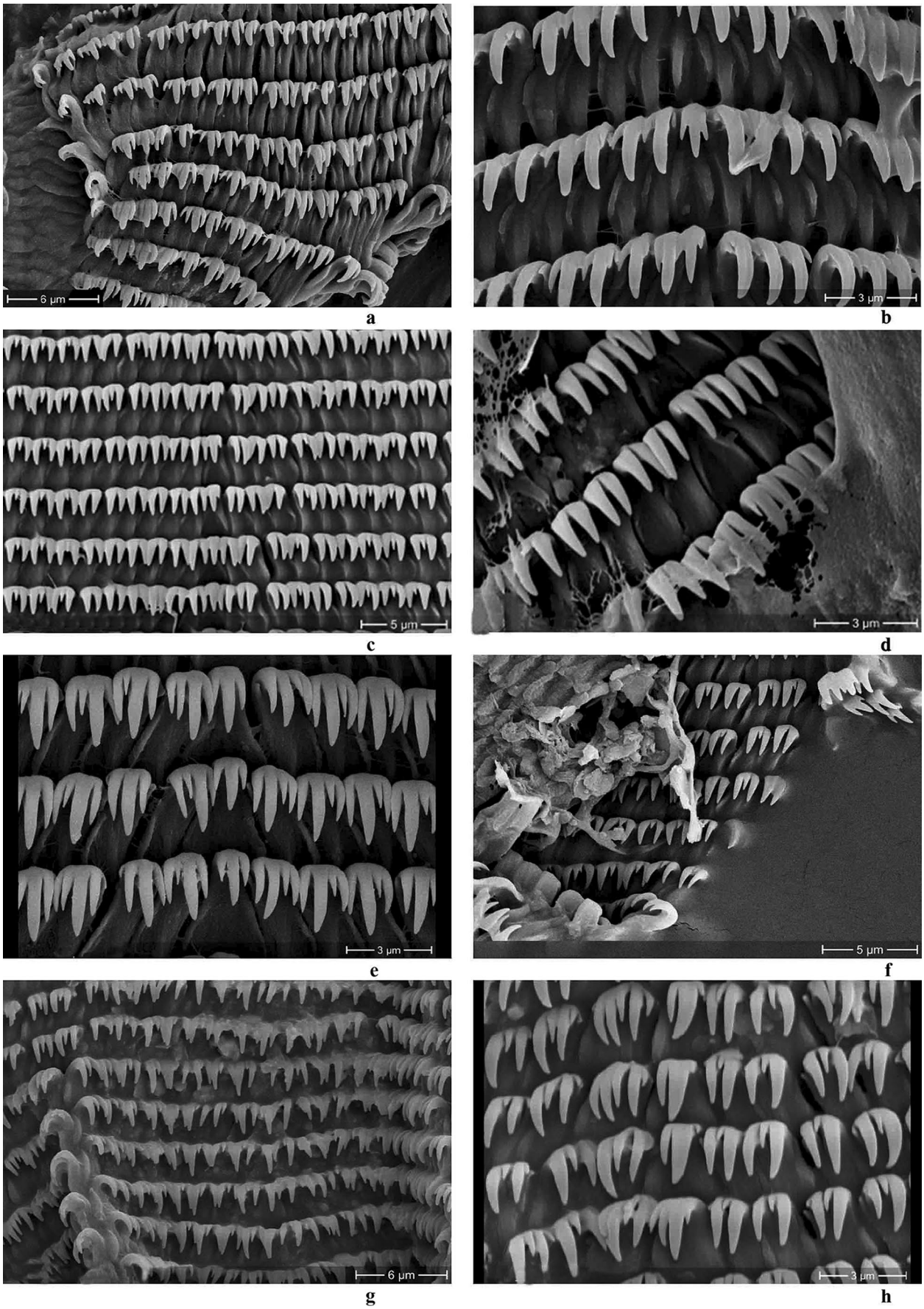
6 µm
a
3 µm
b
5 µm
c
3 µm
d
3 µm
e
5 µm
f
6 µm
g
3 µm
h

◂**Fig. 15** Scanning electron micrographs (SEM) showing transverse rows of dentition on Dinaride *Zospeum* and *Iberozospeum* radulae; (**a**) *Z. pretneri*, (NMBE 553290), Gornja Cerovačka pećina, Croatia, transverse rows of teeth on long, slender basal plates (bp), rachidian (r) and lateral teeth (l), arrows indicate medial grooves on mesocones of individual teeth; (**b**) *Z. isselianum*, NMBE 553389, Turjeva jama, Slovenia, ibid.; (**c**) *Iberozospeum* sp. (RMNH.MOL.234,116), Cueva a Sul, straight transverse rows of small, seemingly bi-cuspid lateral teeth (l) with reduced mesocones on compact basal plates; (**d**) ibid., close up view of rachidian teeth (r), lateral fang-like teeth (l) and transitional teeth (t); (**e**) *I. vasconicum*, (AJC 1848), Cueva Ermita de Sandaili, rachidian teeth (r) flanked by 4-cuspid lateral teeth (l), *C. ibazoricum*-like in form; (**f**) *Iberozospeum* sp. (RMNH.MOL.234108), Cueva la Torcona, lateral teeth showing reduced mesocones (me) flanked by long, fang-like endo- and ectocones (e), rachidian tooth (r) (flipped over in upper righthand corner of image); (**g**) *I. zaldivarae* (AJC 1876a), Cueva de Las Paúles, transverse rows of teeth showing varying cusp lengths; (**h**) ibid., close up view (left to right) of marginal (m) and transitional teeth (t) on short, compact basal plates (bp). — Magnification varies for each perspective, see scale bars; all Figs taken by M. Ruppel, (ret.) Goethe University Frankfurt am Main

enhanced by the tendency towards increased length (i.e. double the ribbon length below the adhesive zone in those of the Pyrenean-Cantabrian individuals), the further westward (i.e. Asturias) the individuals were found, albeit the exception found in Burgos (RMNH.MOL.234108) (Fig. 14h). The radula of topotypic *I. vasconicum* (Fig. 14c) from the more eastern province of Gipuzkoa, for example, shows a moderately long ribbon in comparison to the exceptionally long ribbons extracted from individuals from Asturias and the one from Burgos. Moreover, since the radula is tensioned and moved over the muscular odontophore by muscles that derive from the buccal mass, radular ribbon form is a reflection of these muscles operating the odontophore and radula in concert. In addition, since the odontophore is moved by muscles extending from the body wall and the columellar muscle (in shelled pulmonates) (Luchtel et al., 1997), it is apparent here that *Iberozospeum* has a different muscle constitution (i.e. muscles and modified muscle cells operating the odontophore, the odontophore itself and the columellar muscle) than *Zospeum*. This situation is revealed here by the presence of crystallographic structure on specific points of muscle adhesion on the columellar lamellae in shells of *Iberozospeum* (Fig. 13). Our observation is in sync with the trend in the Ellobiidae (Barker, 2001) that the columellar muscle becomes detached from the body wall from its origin on the columella and has become largely free in the haemocoel. Moreover, the dense, localized surface structure most probably provides traction for the columellar muscle. On a side note, but worth mentioning in context, is that during the manual preparation for SEM, ribbons from *Iberozospeum* mounted especially easily, like laying a carpet, onto the prepared SEM stub. Those of the eastern Alpine and Dinaride taxa, as well as from some *Carychium* species (AJ unpubl. data), tended to be generally more difficult to mount due to their flopping over and furling at the sides during the mounting procedure. This difference may be due to mineral composition or quality of the flexible chitin comprising the ribbon or to potential material thinness due to different or enhanced muscular action on the radular membrane in situ. In contrast to the long and broadly straight version of the Iberian taxa, the radular ribbons of the studied Alpine and Dinaride species are long and narrow and tapered on the anterior end and sometimes, on both ends (i.e. *Z. isselianum* and *Z. frauenfeldii*) (Inäbnit et al., 2019). We consider the consistency in shape, length, broadness and the straight-edged base of the radular ribbon systematically significant in *Iberozospeum*.

Ecologically, the westernmost *Iberozospeum* in our radula study were collected from caves characterised by certain aquatic biotopes (Notenboom & Meijers, 1985). These biotopes included influent caves (Cueva de Rales, Prov. Oviedo (now Asturias)) and temporal effluent caves (Cueva de la Foz, Cueva a Sul, Prov. Oviedo (now Asturias)), and caves with pools, puddles or gours (Cueva la Torcona, Prov. Burgos) or a combination of the latter two (Cueva la Torcona). These ecological situations play a role in diet and substrate composition as well as in the density of mud comprising *Iberozospeum* habitats (Jochum et al., 2012). As for the observed differences in *Iberozospeum*'s radular morphology, Jochum et al. (2015b) considered that the cusps of the radular teeth in *Z. isselianum* (Fig. 15b) interacted with substrate composition and structure (i.e. grain), causing adaptive moderations of morphological detail to evolve and correlate with substrate grain. In the case of *Iberozospeum*, it is probable that the longer, seemingly bi-cuspid lateral teeth of the westernmost sampled populations may well reflect environmentally induced adaptive factors in caves of the westernmost part of *Iberozospeum*'s range. We remark that these westernmost populations were not included in the molecular analyses comprising our study, but rather, collected by Jos Notenboom in 1983–1984 during a study of groundwater fauna in caves of northern Spain (Notenboom & Meijers, 1985).

The radiation of *Iberozospeum* aligns into the bigger context of Iberian geological and evolutionary considerations for which the southern peninsulas of Europe served as major refugia during the Pleistocene glaciation (Hewitt, 2004). Moreover, the Iberian Peninsula has been associated with climate stability over geologic time and is considered to be a historically climate-stable region encompassing high species diversity and endemism (Abellán & Svenning, 2014). Specifically, our study underscores the considerations of Abellán and Svenning (2014), in that the repeated range contractions and expansions experienced during the Pleistocene climatic oscillations may have resulted in the generation of multiple isolated lineages of fauna (in this case, *Iberozospeum*) in

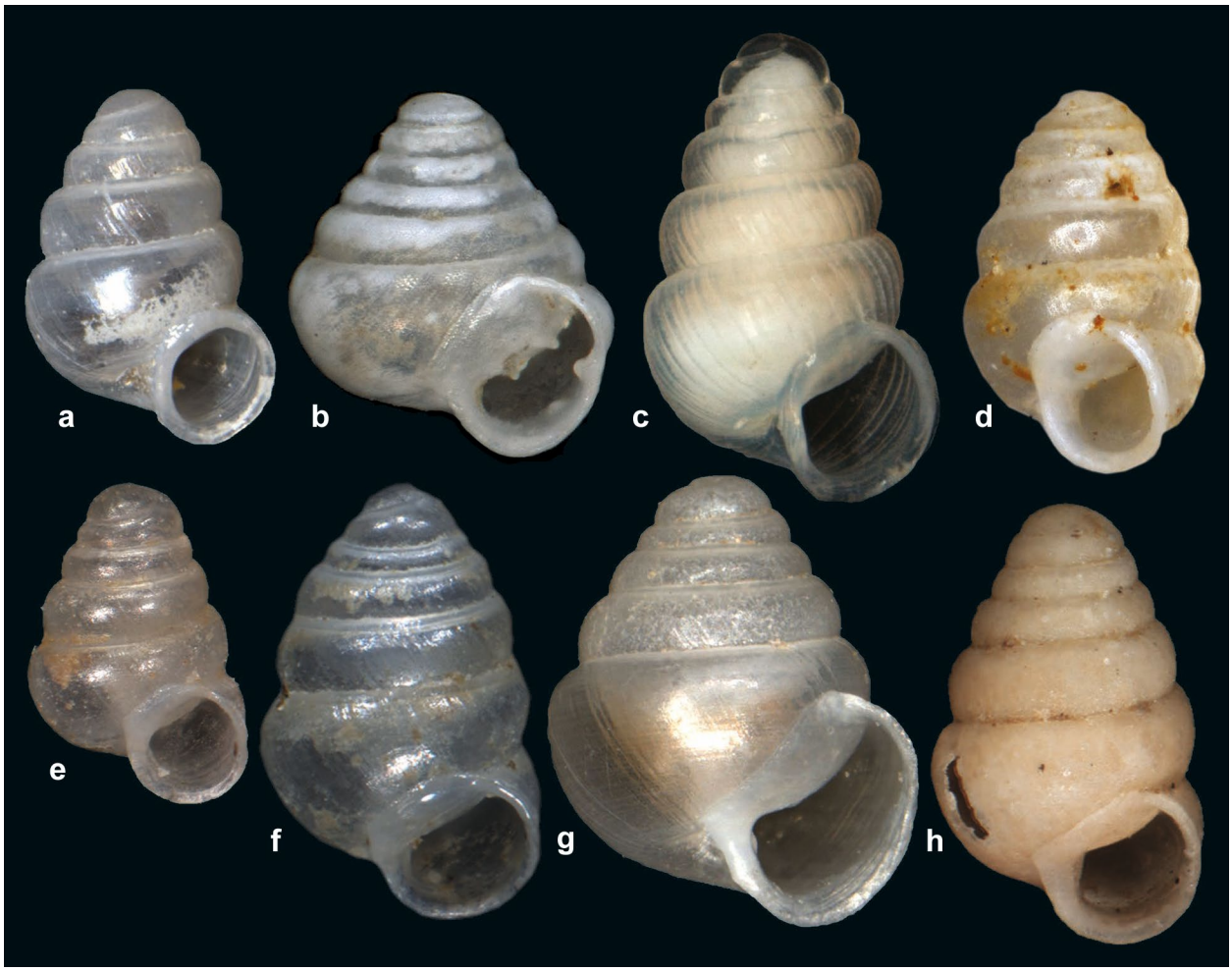

Fig. 16 Type specimens of species of *Iberozospeum*; (**a**) holotype *I. vasconicum* (Prieto et al., 2015 in Jochum et al., 2015a), Gipuzkoa, Cueva de la Ermita de Sandaili, MNCN15.05/60147H, sh: 1.2 mm; (**b**) paratype *I. biscaiense* (Gómez & Prieto, 1983), RMNH.MOLL.334913, Urkizu, Yurre, Cueva de Otxas, sh: ca. 1.23 mm (imaged by Ton de Winter); (**c**) holotype *I. percostulatum* (Alonso et al., 2018), Asturias, Llanes, Cueva de La Herrería, MNCN 15.05/200017H, sh: 1.58 mm; (**d**) lectotype *I. schaufussi* (von Frauenfeld, 1862), "Spain", NHMW 71,837, sh: 1.3 mm; (**e**) holotype *I. praetermissum* (Jochum et al., 2019), Asturias, Cueva del Puente de Inguanzo, RMNH.MOL.55391, sh: 1.08 mm; (**f**) paratype *I. bellesi* (Gittenberger, 1973), Huesca, Cueva del Molino de Aso, RMNH.Mol.234,137, sh: 1.49 mm (imaged by Ton de Winter); (**g**) holotype *I. zaldivarae* (Prieto et al., 2015 in Jochum et al., 2015a), Burgos, Cueva de Las Paúles, MNCN 15.05/60148H, sh: 1.52 mm; (**h**) holotype *I. gittenbergeri* (Jochum et al., 2019), Asturias, Cueva del Puente de Inguanzo, RMNH.MOL.234166, sh: 1.49 mm

different refugial areas. The Cantabrian and Pyrenees Mountains, harbouring labyrinthine cave systems, well serve as current refugial areas for *Iberozospeum* species that may have been more widespread during colder periods during the Pleistocene. Moreover, with the Pyrenees-Cantabrian Mountains running east–west together with the main rivers flowing along a north–south axis, the following scenario can be proposed considering climatic, geological and physiographical characteristics of this geologically younger part of Spain (Notenboom & Meijers, 1985): *Iberozospeum* could have survived and spread via altitudinal shifts as cave systems gave way and sank into each other due to geologic processes and groundwater mechanisms, allowing the distribution of species and sympatry of species to occur over time.

Taxonomic implications

We found a well-supported, two-clade system in the genus *Zospeum* (Figs. 2 and 3) and propose here a new genus encompassing the northern Spanish radiation.

Genus ***Iberozospeum*** Jochum, Kneubühler, Prieto and Neubert, n. gen.

Type species *Zospeum zaldivarae* (Prieto et al., 2015 in Jochum et al., 2015a).

Differential diagnosis *Iberozospeum*, n. gen., differs from *Zospeum* by the generally smaller shell (on the average ca. 1.2 mm). The radula ribbon differs by its greater length,

Table 4 Investigated sympatric *Iberozospeum* species living in Spanish caves

Cave	Species 1	Species 2
Herrería	NMBE 557253 *praetermissum* (purple clade)	NMBE 557136 *percostulatum* (green clade)
Irutxin	NMBE 557238 *biscaiense* (grey clade)	NMBE 557221 *vasconicum* (light blue clade)
Las Paules	No. 162 and 163 Weigand 2013 *zaldivarae* (grey clade)	NMBE 557178 and NMBE 557244 *vasconicum* (light blue clade)
Otxas	NMBE 557240 *biscaiense* (grey clade)	NMBE 557223 *vasconicum* (pink clade)
Valdemora	NMBE 557246 *praetermissum* (purple clade)	NMBE 557247 *gittenbergeri* (green clade)

regular broadness below the adhesive zone and its perfectly straight base. Radular teeth are smaller and more numerous per transverse row. The basal plates are more compact and shorter than the long, narrow versions in *Zospeum* species. At the microstructural level, it differs by localized, dense, rough, overlapping wedge-like scales of crystallographic structure on the surface of the columellar lamellae. These sites are located only at the points of contact with the columellar muscle. It also appears to differ by the correlating, vascularized humps of columellar muscle to the corresponding zones of microstructural texture on the lamellae.

Etymology The name *Iberozospeum* derives from combining the region of origin of the type species, the Iberian Peninsula, and the generic name of *Zospeum* (Bourguignat, 1856).

Included taxa: all hitherto known species from the Iberian Peninsula:

Iberozospeum schaufussi (von Frauenfeld, 1862).
Iberozospeum bellesi (Gittenberger, 1973).
Iberozospeum biscaiense (Gómez & Prieto, 1983).
Iberozospeum vasconicum (Prieto et al., 2015 in Jochum et al., 2015a).
Iberozospeum zaldivarae (Prieto et al., 2015 in Jochum et al., 2015a).
Iberozospeum percostulatum (Alonso et al., 2018).
Iberozospeum praetermissum (Jochum et al., 2019).
Iberozospeum gittenbergeri (Jochum et al., 2019).

Iberozospeum costulatum Prieto and Jochum, n. sp.

Type locality Mina del Pedreo (Bizkaia: Arcentales; 43.26800 -3.21402, 440 m).

Holotype A shell of 1.43 mm [MNCN 15.05/200128, ex. ZUPV 1952]; 22.02.2014, C. Prieto, A. Calvo, P. Jiménez leg.

Paratypes Mina del Pedreo [type locality]; 22.02.2014, C. Prieto, A. Calvo, P. Jiménez leg. [ZUPV 1952: 2 shells + 2 juvenile shells] 31.08.2014, C. Prieto, A. Calvo leg. [ZUPV 2578: 15 shells + 3 juvenile shells, ZUPV 2583: 1 shell] [MNCN 15.05/200129: 5 shells]. Cueva de Valdebeci (Bizkaia: Sopuerta: Beci; 43.24516 -3.17316, 188 m); 20.10.2015, A. Calvo leg. [ZUPV 3078: 6 shells] [NMBE 557231: 1 specimen, sequenced; Fig. 11c]. Cueva de Cuvias Negras (Cantabria: Soba: Asón; 43.25132 -3.60688, 250 m); 12.04.2017, C. Prieto, S. Quiñonero, A. Alonso, J. Ruiz-Cobo leg. [ZUPV 4714: 38 shells + 2 specimens] [NMBE 557227: 1 specimen, sequenced; Fig. 11b; NMBE 568196: 5 shells] [SMF 349,424: 5 shells] [MHNG-MOLL-0137391: 5 shells] [MNCN 15.05/200130: 10 shells] [CAA·w/o nº: 19 shells] [CSQS·w/o nº: 25 shells].

Other material Cueva del Cesáreo (Cantabria: Liérganes: Extremera; 43.32034 -3.72279, 258 m); 21.03.2016, S. Quiñonero, J. Ruiz-Cobo, A. Alonso leg. [ZUPV 3807: 3 shells] [CAA·w/o nº: 1 shell] [NMBE 559626: 2 specimens, sequenced; Fig. 11a]. Cueva de Asunción (Cantabria: Ramales de la Victoria: Guardamino; 43.25837 -3.44820, 180 m); 21.03.2016, S. Quiñonero, J. Ruiz-Cobo leg. [ZUPV 3808: 4 shells]. Cueva del Comellante (Cantabria: Ruesga; 43.31111 -3.60806, 170 m); 30.03.2015, S. Quiñonero, J. Ruiz-Cobo leg [ZUPV 3804: 1 shell] [CSQS·w/o nº:3 shells]. Cueva de Covallarco (Cantabria: San Roque de Riomiera: Merilla; 43.25654 -3.73412, 402 m); 18.06.2016, CP, J. Fernández leg. [ZUPV 3974: 1 shell]. Cueva de Cullalvera (Cantabria: Ramales de la Victoria; 43.25577 -3.45808, 95 m); 19.09.2014, C. Prieto, A. Calvo leg. [ZUPV 2604: 1 shell]. Torca de El Porrón (Cantabria: Ruesga: Porracolina; 43.25111 -3.66356, 920 m); 09.09.2016, M. Gutiérrez leg. [ZUPV 4180: 1 shell]. Cueva de La Puntida (Cantabria: Miera: Ajanedo; 43.25883 -3.71042, 500 m); 12.10.2015, C. Prieto, A. Calvo leg. [ZUPV 3032: 90 shells] [CSQS·w/o nº: 10 shells]. Fuente de La Revilla (Cantabria: Voto: San Miguel de Aras; 43.31972 -3.52036, 55 m); 30.03.2015, S. Quiñonero leg. [ZUPV 3806: 3 shells]. Cueva de Las Cascajosas (Cantabria: San Roque de Riomiera; 43.25457


a
b
c
d
e
f
g
h
i
j
k
l

◂**Fig. 17** *Iberozospeum costulatum* n. sp. (**a**–**e**) holotype, 1.43 mm height [MNCN 15.05/200128, ex. ZUPV 1952], Mina del Pedreo (Bizkaia: Arcentales; 43.26800 -3.21402, 440 m). (**f**–**g**) paratype shells from the type locality [ZUPV 1952, F: juvenile shell, G: shell of 1.51 mm height. (**h**–**i**) no paratype shell of 1.48 mm height [ZUPV 3807] from Cueva del Cesáreo (Cantabria: Liérganes: Extremera; 43.32034 -3.72279, 258 m). (**j**–**k**) paratype shells from Cueva de Cuvias Negras (Cantabria: Soba: Asón; 43.25132 -3.60688, 250 m) [CSQS·w/o nº]. (**l**) no paratype shell from Cueva del Cesáreo [CSQS·w/o nº]. Photos a–i by Carlos Prieto; j–l by Sergio Quiñonero and Álvaro Alonso

-3.71924, 328 m); 09.03.2018, C. Prieto, J. Ruiz-Cobo leg. [ZUPV 5154: 2 shells]. Cueva del Molino de la Peña (Cantabria: Rasines; 43.29101 -3.36840, 180 m); 04.08.2013, S. Quiñonero, J. Ruiz-Cobo leg. [ZUPV 3802: 2 shells, broken]. Sima PO-153 (Cantabria: San Roque de Riomiera: Porracolina; 43.22984 -3.69050, 585 m); 08.10.2016, M. Gutiérrez leg. [ZUPV 4184: 4 shells]; 12.11.2016, C. Prieto, M. Gutiérrez, J. A. Noriega leg. [ZUPV 4203: 20 shells]. Sima PO-27 (Cantabria: Miera; 43.24695 -3.67023, 910 m); 07.05.2016, M. Gutiérrez leg. [ZUPV 3822: 8 shells]. Cueva de San Juan de Socueva (Cantabria: Arredondo: Socueva; 43.26671 -3.61339, 430 m); 12.04.2017, C. Prieto, S. Quiñonero, A. Alonso, J. Ruiz-Cobo leg. [ZUPV 4722: 12 shells].

Etymology The specific epithet derives from the well-defined ribbing of the last whorls of the shell.

Diagnosis A medium-sized (average, 1.35 mm, $n=52$) and wide (average, 0.76 mm, $n=52$) *Iberozospeum* species with convex whorls bearing well-defined ribs, oblique, reniform aperture with broad straight-edged parietal callus and a strong columellar lamella clearly seen inside the aperture.

Description (Fig. 17). Shell of medium size (1.24–1.55 mm, $n=52$, holotype, 1.43 mm), ovate conical. Spire formed by five (4.6–5.9, n = 52) rather convex whorls separated by a deep suture. Protoconch (nucleus, 0.175 mm wide) and apical whorls smooth (Fig. 17f) with teleoconch bearing regularly spaced (5–6/0.5 mm; 27 in the body whorl, n = 52), well-defined ribs, extending from one whorl to the next; ribs of the hind peristome region are more densely aligned and thinner. Body whorl large (holotype, 60% of the shell height), with upper convexity, ascending behind the aperture. Umbilicus closed, with ribs reaching the umbilical cavity. Aperture reniform, obliquely transverse (holotype, 47% of the shell height), attached to the body whorl by a thickly callused, broad, straight-edged parietal callus. Peristome wide and reflexed; lateral and palatal side regularly arched; columellar side almost straight and vertical. Inner lamella singular, large, oblique, (Fig. 17g) located above the parieto-columellar junction; lamella visible in oblique apertural view (Fig. 17c). Shell surface with micro sculpture of irregular spiral striae.

Geographical distribution *Iberozospeum costulatum* n. sp. inhabits caves throughout western Bizkaia and the eastern part of Cantabria (Fig. 18). In Bizkaia, *I. costulatum* is known from two caves located 4.2 km apart: Mina del Pedreo, where it was first discovered, and Cueva de Valdebeci (holotype, sequenced population). Both caves belong to the same limestone formation (Alén-Lujar) cut by the Barbadun river. The remaining localities are in Cantabria. They are separated from the Bizkaian caves by a distance of 20 km, with Cueva Cullalvera and Cueva de Asunción being the nearest. All Cantabrian localities are located in the limestone massifs belonging to the Miera and Asón river basins with Cueva del Cesáreo (sequenced, Fig. 11a) constituting the most north-western cave separated from this central block. We remark that *I. costulatum* appears to be sympatric with *I. biscaiense* in the Montes de Triano massif west of Bilbao (Prieto & Calvo 2013; unpublished records) and that the east-westward geographic span recorded for *I. costulatum* likely represents the true geographic distribution of this species.

Variability Ribbing is the most conspicuous feature on the shell of *I. costulatum*. Although the shells from the same cave show similar rib strength, spacing and length, a notable spectrum of variability is present in different cave populations. Shells deriving from populations from the Miera upper basin, such as La Puntida, PO-153 or Cuvias Negras (Fig. 17j–k), show poorly developed ribs and a weak columellar lamella, while individuals from Fuente de La Revilla bear strong and irregular ribs. On the other hand, shells from Asunción have well separated ribs (5/0.5 mm). Although obscured by wide intra-populational variation, shell size also varies between populations. Shells from Cuvias Negras are the smallest and those from Valdebeci are the largest. The inner columellar lamella also varies somewhat in form in shells from Cueva de Cesáreo, whereby in addition to the columellar lamella, a small basal lamella can be seen from the opening in oblique view (Fig. 17h–i).

Remarks The conspicuous ribbing differentiates *I. costulatum* from all other iberozospeid taxa except *I. percostulatum*. The shell of *I. percostulatum* is higher (1.34–1.80 mm, average 1.55 mm) and narrower (1.32–1.65 mm, average 1.51 mm, $n=42$) and lacks inner lamellae (Alonso et al., 2018). Additionally, their geographic ranges are 80 km apart.

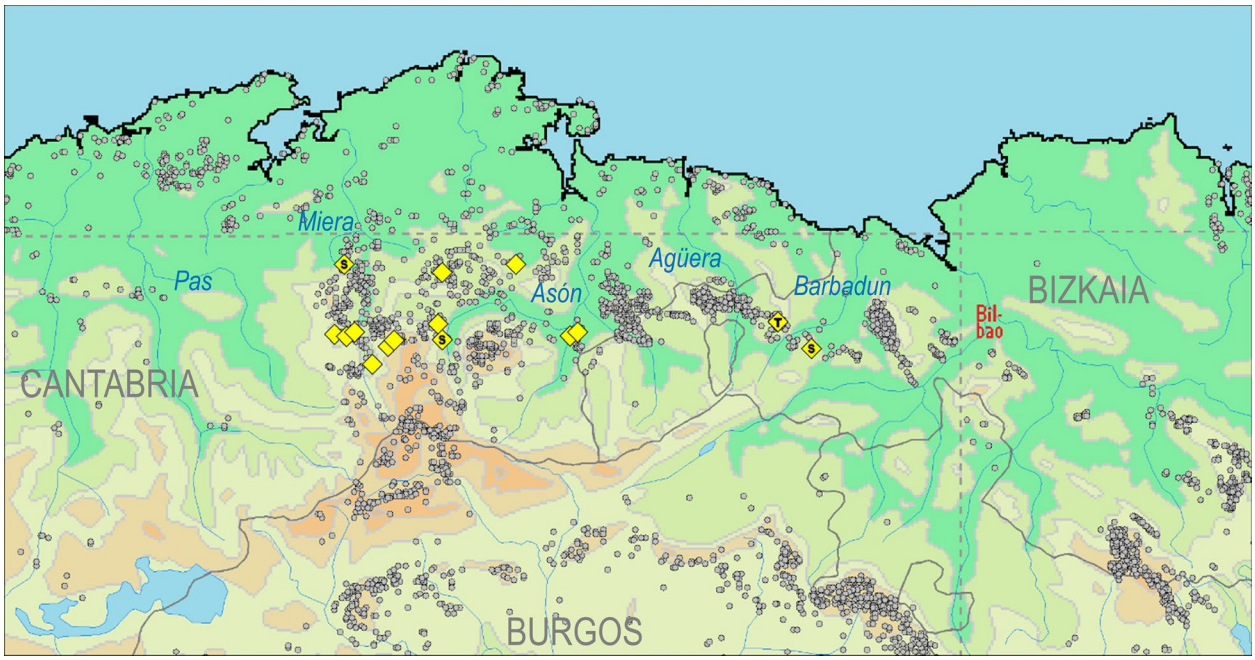

Fig. 18 Geographical distribution of *Iberozospeum costulatum* n. sp. The type locality and sequenced populations are indicated by T and S, respectively

Conclusion

In this integrative study, we investigated 57 populations of cavernicolous zospeid snails using genetic and morphological data. Our study revealed a separate radiation for species inhabiting northern Spanish caves for which the new genus, *Iberozospeum*, has been defined. *Iberozospeum* populations show on-going speciation in situ within isolated cave systems of northern Spain. Our investigations corroborated the proposed ancestral area reconstruction of Weigand et al. (2013) indicating that the "Cantabrian Mountains + Alps" or "Cantabrian Mountains + Dinaric Alps" was the ancestral area of the *Iberozospeum* radiation. Coherent mitochondrial and nuclear sequence patterns as well as common morphological traits were observed in most of the clades. Three new species were molecularly revealed and one, *Iberozospeum costulatum*, is described using additional morphological data.

Our comparative histological investigations revealed the huge size of the albumen gland for the first time in a sexually mature member in the female phase within the subterranean Carychiidae. We found significant morphological and structural differences in both the columellar muscle and the radulae of Dinaride *Zospeum* and *Iberozospeum* species. SEM investigations of the radular ribbon reveal that dentition form, size and alignment, consistency in ribbon shape, length, broadness and the straight-edged base are systematically significant in *Iberozospeum* species and that it morphologically differentiates these species from those of the Eastern Alpine and Dinaride *Zospeum* taxa.

Our investigations are ongoing. Future collection efforts and phylogeographic investigations will do well to reveal deeper patterns of phylogenetic relatedness and evolutionary processes in *Iberozospeum* populations.

Supplementary Information The online version contains supplementary material available at https://doi.org/10.1007/s13127-021-00517-9.

Acknowledgements We gratefully acknowledge Anton J. de Winter for his einsatz and insights in an earlier project and for kindly allowing AJ access to the Jos Notenboom Collection at the Naturalis Biodiversity Center (Leiden, NL). We are indebted to Alvaro Alonso Suárez, X. Azkoaga, Alfonso Calvo, J. M. Expósito, Jon Fernández, Marta Gutierrez, Jagoba Malumbres, Javi Moreno, Sergio Quiñonero-Salgado, Jesús Ruiz-Cobo and Pantxo Zuazu for their tremendous collecting efforts, encompassing 55 caves. We gratefully acknowledge Claudia Nesselhauf (ret. Goethe University, Frankfurt, Germany) for her extreme patience and skill in extracting radulae from these miniscule snails and to Gabi Elter (Goethe University, Frankfurt, Germany) who prepared the histological sections of *I. vasconicum*. We thank Dirk Vendermarel (Naturalis Biodiversity Center) and Manfred Ruppel (ret.) (Goethe University, Frankfurt, Germany) for their insights and expertise at the SEM. We are grateful to Thomas Inäbnit for his input and technical support and Alexander M. Weigand for earlier discussions. We are indebted to Annette Kolb (former Klussmann-Kolb) for her long-term support of this work as well as to Dorian Dörge (Goethe University, Frankfurt Germany), who imaged the multitude of histological slides. AJ received support via grants from The Malacological Society of London and the SYNTHESYS Project http://www.synthesys.info/, which is financed by the European Community Research Infrastructure Action under the FP7 "Capacities" Program.

Funding Open Access funding provided by Universität Bern. Funding for genetic analyses came from the Natural History Museum Bern, Bern, Switzerland.

Data availability All data is published in the manuscript. Sequences are deposited in Genbank.

Code availability Software and programs are cited in the manuscript.

Declarations

Ethics approval Not applicable.

Consent for publication We give permission for the following paper to be published in Organisms Diversity & Evolution.

Conflict of interest Not applicable.

References

Abellán, P., & Svenning, J.-C. (2014). Refugia within refugia – patterns in endemism and genetic divergence are linked to Late Quaternary climate stability in the Iberian Peninsula. *Biological Journal of the Linnean Society, 113*(1), 13–28. https://doi.org/10.1111/bij.12309

Alonso, A., Prieto, C. E., Quiñonero-Salgado, S., & Rolán, E. (2018). A morphological gap for Iberian *Zospeum* filled: *Zospeum percostulatum* sp. n. (Gastropoda, Eupulmonata, Carychiidae) a new species from Asturias (Spain). *Subterranean Biology, 25,* 35–48. https://doi.org/10.3897/subtbiol.25.23364

Altekar, G., Dwarkadas, S., Huelsenbeck, J. P., & Ronquist, F. (2004). Parallel Metropolis-coupled Markov chain Monte Carlo for Bayesian phylogenetic inference. *Bioinformatics, 20,* 407–415.

Bank, R. A., & Gittenberger, E. (1985). Notes on Azorean and European *Carychium* species (Gastropoda, Basommatophora, Ellobiidae). *Basteria, 49*(4/6), 85–100.

Barker, G. M. (2001). *The Biology of Terrestrial Mollusks* (p. 558). CABI Publishing.

Bole, J. (1960). Novi vrsti iz rodu *Zospeum* Bourg. (Gastropoda). *Biološki Vestnik, 7,* 61–64.

Bole, J. (1974). Rod *Zospeum* Bourguignat 1865 (Gastropoda, Ellobiidae) v Jugoslawiji. *Razprave Slovenska Academija znanosti in Umetnosti Cl.* IV, 17(5), 249–291.

Bouaziz-Yahiatene, H., Pfarrer, B., Medjdoub-Bensaad, F., & Neubert, E. (2017). Revision of *Massylaea* Möllendorff, 1898 (Stylommatophora, Helicidae). *ZooKeys 694*, 109–133. https://doi.org/10.3897/zookeys.694.15001

Bourguignat, J. R. (1856). Aménités malacologiques. Du genre *Zospeum*. *Revue et Magasin de Zoologie pure et appliquée (2)*8, 499–516.

Colgan, D., McLauchlan, A., Wilson, G. D. F., Livingston, S. P., & Edgecombe, G. D. (1998). Histone H3 and U2 snRNA DNA sequences and arthropod molecular evolution. *Australian Journal of Zoology, 46,* 419–437.

Dörge, D. (2010). Vergleich der Anatomie und Histologie zweier Mikroschneckenarten, *Carychium minimum* Müller, 1774 und *Zospeum isselianum* Pollonera, 1887 (Gastropoda, Pulmonata, Ellobiidae). *Unpublished BSc thesis*, Goethe-University, Frankfurt am Main, Germany.

Folmer, O., Black, M., Hoe, W., Lutz, R., & Vrijenhoek, R. (1994). DNA primers for amplification of mitochondrial cytochrome c oxidase subunit I from diverse metazoan invertebrates. *Molecular Marine Biology and Biotechnology, 3*(5), 294–299.

Freyer, H. (1855). Über neu endeckte Conchylien aus den Geschlechtern Carychium und Pterocera. *Sitzungsberichte der mathematisch-naturwissenschaftlichen Classe der kaiserlichen Akademie der Wissenschaften 5*, 18–23.

Gittenberger, E. (1973). Eine *Zospeum*-Art aus den Pyrenäen Zospeum Bellesi Spec. Nov. *Basteria, 37*(5–6), 137–140.

Gittenberger, E. (1980). Three Notes on Iberian Terrestrial Gastropods. *Zoologische Mededelingen, 55*(17), 201–213.

Gómez, B. J., & Prieto, C. E. (1983). *Zospeum biscaiense* nov. sp. (Gastropoda, Ellobiidae) otro molusco troglobio para la Península Ibérica. *Speleon, 26–27,* 7–10.

Harry, H. W. (1997–1998). *Carychium exiguum* (Say) of lower Michigan; Morphology, Ecology, Variation and Life History (Gastropoda, Pulmonata). *Walkerana 9*(21), 104

Hewitt, G. M. (2004). Genetic consequences of climatic oscillations in the Quaternary. *Philosophical Transactions of the Royal Society of London B: Biological Sciences, 359,* 183–195. https://doi.org/10.1098/rstb.2003.1388

Holznagel, W. E. (1998). A nondestructive method for cleaning gastropod radulae from frozen, alcohol-fixed, or dried material. *American Malacological Bulletin, 14,* 181–183.

Huelsenbeck, J. P., & Ronquist, F. (2001). MRBAYES: Bayesian inference of phylogeny. *Bioinformatics, 17,* 754–755.

Inäbnit, I., Jochum, A., Kampschulte, M., Martels, G., Ruthensteiner, R., Slapnik, R., Nesselhauf, C., & Neubert, E. (2019). An integrative taxonomic study reveals carychiid microsnails of the troglobitic genus *Zospeum* in the Eastern and Dinaric Alps (Gastropoda, Ellobioidea, Carychiinae). *Organisms Diversity and Evolution, 19,* 135–177. https://doi.org/10.1007/s13127-019-00400-8

Jochum, A. (2011). Evolution and diversity of the troglobitic Carychiidae–A morphological and phylogenetic investigation of the terrestrial ellobioid genera, *Carychium* and *Zospeum*. *The Malacologist, 57,* 16–18.

Jochum, A., Weigand, A. M., Slapnik, R., Valentinčič, J., & Prieto, C. P. (2012). The microscopic ellobioid, *Zospeum* Bourguignat, 1856 (Pulmonata, Ellobioidea, Carychiidae) makes a big debut in Basque Country and the province of Burgos (Spain). *MalaCo 8*, 400–403. http://www.journal-malaco.fr

Jochum, A., de Winter, A. J., Weigand, A. M., Gómez, B. J., & Prieto, C. E. (2015a). Two new species of *Zospeum* Bourguignat, 1856 from the Basque-Cantabrian Mountains, Northern Spain (Eupulmonata, Ellobioidea, Carychiidae). *ZooKeys, 483,* 81–96. https://doi.org/10.3897/zookeys.483.9167

Jochum, A., Slapnik, R., Klussmann-Kolb, A., Páll-Gergely, B., Kampschulte, M., Martels, G., Vrabec, M., Nesselhauf, N., & Weigand, A. M. (2015b). Groping through the black box of variability: An integrative taxonomic and nomenclatural re-evaluation of *Zospeum isselianum* Pollonera, 1887 and allied species using new imaging technology (Nano-CT, SEM), conchological, histological

and molecular data (Ellobioidea, Carychiidae). *Subterranean Biology, 16,* 123–165. https://doi.org/10.3897/subtbiol.16.5758

Jochum, A., Neubauer, T. A., & Harzhauser, M. (2015c). Microstructural details in shells of the gastropod genera *Carychiella* and *Carychium* of the Middle Miocene. *Lethaia, 49,* 87–101. https://doi.org/10.1111/let.12134

Jochum, A., Prieto, C. E., Kampschulte, M., Martels, G., Ruthensteiner, B., Vrabec, M., Dörge, D. D., & de Winter, A. J. (2019). Re-evaluation of *Zospeum schaufussi* von Frauenfeld, 1862 and *Z. suarezi* Gittenberger, 1980, including the description of two new Iberian species using Computer Tomography (CT) (Eupulmonata, Ellobioidea, Carychiidae). *ZooKeys, 835,* 65–86. https://doi.org/10.3897/zookeys.835.33231

Kruckenhauser, L., Plan, L., Mixanig, H., & Slapnik, R. (2019). Verwandtschaftsbeziehungen von Kärntner Populationen der Höhlenschnecke *Zospeum isselianum*. *Die Höhle, 70*(1–4), 139–147.

Kumar, S., Stecher, G., Li, M., Knyaz, C., & Tamura, K. (2018). MEGA X: Molecular Evolutionary Genetics Analysis across computing platforms. *Molecular Biology and Evolution, 35,* 1547–1549. https://doi.org/10.1093/molbev/msy096

Kuščer, L. (1932). Höhlen- und Quellenschnecken aus dem Flussgebiet der Ljubljanica. *Archiv Für Molluskenkunde, 64*(2), 60–61.

Lanfear, R., Frandsen, P. B., Wright, A. M., Senfeld, T. & Calcott, B. (2016) PartitionFinder 2: new methods for selecting partitioned models of evolution for molecular and morphological phylogenetic analyses. *Molecular biology and evolution*. https://doi.org/10.1093/molbev/msw260

Luchtel, D. L., Martin, A. W., Deyrup-Olsen, I., & Boer, H. H. (1997). *Gastropoda*: *Pulmonata*. In: F. W. Harrison & A. J. Kohn (Eds.) *Microscopic Anatomy of Invertebrates* (vol 6B, pp. 459−718). Mollusca II, Wiley-Liss, Inc., New York.

Maier H. C. (1982). Zur Systematik, Zoogeographie, Anatomie und Biologie der Gattung *Zospeum* BGT. 1856 (Gastropoda: Basommatophora: Ellobiidae) [DPhil thesis] (p. 175). Vienna, Austria: University of Vienna.

Martins, A. M. F. (1996). Anatomy and Systematics of the Western Atlantic Ellobiidae (Gastropoda, Pulmonata). *Malacologia, 37*(2), 163–332.

Martins, A. M. F. (2007). Morphological and anatomical diversity within the Ellobiidae (Gastropoda, Pulmonata, Archaeopulmonata). *Vita Malacologica, 4,* 1–28.

Morton, J. E. (1955). The functional morphology of the British Ellobiidae (Gastropoda, Pulmonata) with special reference to the digestive and reproductive systems. *Philosophical Transactions of the Royal Society of London* 239(B), 89−160.

Notenboom, J., & Meijers, I. (1985). Research on the groundwater fauna of Spain: List of stations and first results. *Verslagen En Technische Gegevens, Institute of Taxonomic Zoology, University of Amsterdam, 42,* 5–37.

Pollonera, C. (1887). Note malacologiche. I. Molluschi della Valle del Natisone (Friuli). *Bullettino della Società Malacologica Italiana*, *12*["1886"], 204−208. http://archive.org/details/bullettino121886soci

Prieto, C. E., & Zuazu, F. J. (2018). New records and geographical distribution of *Zospeum bellesi* Gittenberger 1973 (Gastropoda: Ellobiida: Ellobiidae). *Iberus, 36*(2), 73–79.

Puillandre, N., Lambert, A., Brouillet, S., & Achaz, G. (2012). ABGD, automatic barcode gap discovery for primary species delimitation. *Molecular Ecology, 21,* 1864–1877. https://doi.org/10.1111/j.1365-294X.2011.05239.x

Ronquist, F., & Huelsenbeck, J. P. (2003). MRBAYES 3: Bayesian phylogenetic inference under mixed models. *Bioinformatics, 19,* 1572–1574.

Rossmässler, E. A. (1839). Iconographie der Land- und Süsswasser-Mollusken, mit vorzüglicher Berücksichtigung der europäischen noch nicht abgebildeten Arten. 1: 2 (3/4). Arnoldische Buchhandlung, Dresden, Leipzig, 46.

Simon, C., Frati, F., Beckenbach, A., Crespi, B., Liu, H., & Flook, P. (1994). Evolution, weighting, and phylogenetic utility of mitochondrial gene sequences and a compilation of conserved polymerase chain reaction primers. *Annals of the Entomological Society of America, 87*(6), 651–701.

Stamatakis, A. (2006). RAxML-VI-HPC: Maximum likelihood-based phylogenetic analyses with thousands of taxa and mixed models. *Bioinformatics, 22*(21), 2688–2690. https://doi.org/10.1093/bioinformatics/btl446

von Frauenfeld, G. (1854). Über einen bisher verkannten Laufkäfer beschrieben von L. Miller; und einen neuen augenlosen Rüsselkäfer, beschrieben von F. Schmidt; ferner einige von Schmidt in Schischka neu entdeckte Höhlentiere. *Verhandlungen Des Zoologisch-Botanischen Vereins in Wien, 4,* 23–34.

von Frauenfeld G. (1856). Die Gattung *Carychium*. *Sitzungsberichte der Mathematisch-naturwissenschaftlichen Classe der Kaiserlichen Akademie der Wissenschaften*, *19*(1–2), 70–93, 1 plate. Wien.

von Frauenfeld, G. (1862). Ueber ein neues Höhlen-*Carychium* (Zospeum Brg.) und zwei neue fossile Paludinen. *Verhandlungen der Zoologisch-Botanischen Gesellschaft in Wien, 12*, 969−972. http://www.biodiversitylibrary.org/item/95692#page/487/mode/1up

Weigand, A. M., Jochum, A., Pfenninger, M., Steinke, D., & Klussmann-Kolb, A. (2011). A new approach to an old conundrum – DNA barcoding sheds new light on phenotypic plasticity and morphological stasis in microsnails (Gastropoda, Pulmonata, Carychiidae). *Molecular Ecology Resources, 11,* 255–265. https://doi.org/10.1111/j.1755-0998.2010.02937.x

Weigand, A. M., Jochum, A., Slapnik, R., Schnitzler, J., Zarza, E., & Klussmann-Kolb, A. (2013). Evolution of microgastropods (Ellobioidea, Carychiidae): Integrating taxonomic, phylogenetic and evolutionary hypotheses. *BMC Evolutionary Biology, 13*(1), 18. https://doi.org/10.1186/1471-2148-13-18